

Estimating Fair Graphs from Graph-Stationary Data

Madeline Navarro

*Department of Electrical and Computer Engineering
Rice University
Houston, TX 77005-1827, USA*

NAV@RICE.EDU

Andrei Bucilea

*Department of Signal Theory and Communications
King Juan Carlos University
Madrid, Spain*

ANDREI.BUCIULEA@URJC.ES

Samuel Rey

*Department of Signal Theory and Communications
King Juan Carlos University
Madrid, Spain*

SAMUEL.REY.ESCUDERO@URJC.ES

Antonio G. Marques

*Department of Signal Theory and Communications
King Juan Carlos University
Madrid, Spain*

ANTONIO.GARCIA.MARQUES@URJC.ES

Santiago Segarra

*Department of Electrical and Computer Engineering
Rice University
Houston, TX 77005-1827, USA*

SEGARRA@RICE.EDU

Editor: TBD

Abstract

We estimate *fair graphs from graph-stationary nodal observations* such that connections are not biased with respect to sensitive attributes. Edges in real-world graphs often exhibit preferences for connecting certain pairs of groups. Biased connections can not only exacerbate but even induce unfair treatment for downstream graph-based tasks. We therefore consider group and individual fairness for graphs corresponding to group- and node-level definitions, respectively. To evaluate the fairness of a given graph, we provide multiple bias metrics, including novel measurements in the spectral domain. Furthermore, we propose *Fair Spectral Templates (FairSpecTemp)*, an optimization-based method with two variants for estimating fair graphs from stationary graph signals, a general model for graph data subsuming many existing ones. One variant of FairSpecTemp exploits commutativity properties of graph stationarity while directly constraining bias, while the other implicitly encourages fair estimates by restricting bias in the graph spectrum and is thus more flexible. Our methods enjoy high probability performance bounds, yielding a *conditional* tradeoff between fairness and accuracy. In particular, our analysis reveals that *accuracy need not be sacrificed to recover fair graphs*. We evaluate FairSpecTemp on synthetic and real-world data sets to illustrate its effectiveness and highlight the advantages of both variants of FairSpecTemp.

Keywords: Graph estimation, fairness, group fairness, graph signal processing, graph learning

1 Introduction

Due to their well-understood properties yet rich modeling capacity, graphs have become a staple tool for interconnected data in many disciplines (Kolaczyk, 2009; Ortega et al., 2018; Marques et al., 2020; Djuric and Richard, 2018). A graph itself may be of interest for analysis, for example, to assess social interactions (Farine and Whitehead, 2015), or it can be used for tasks such as improving recommendations (Duricic et al., 2023; Mansoury et al., 2022) or modeling epidemic spread (Achterberg et al., 2022). In addition to classical fields, graph neural networks (GNNs) and other graph-based machine learning tools have enjoyed ample research to process complex data for challenging tasks (Wu et al., 2021).

In many cases, the graph of interest is unavailable, and we must instead build its connections from data that reflects the underlying pairwise relationships (Brugere et al., 2019). Sensitive yet critical applications include identifying correlations between financial institutions (Franzolini et al., 2024), predicting pairwise connections between neurons or genes (Yatsenko et al., 2015; Cai et al., 2013), and tracking movement for contact tracing (Chang et al., 2021). Some estimate graphs to aid another task, which includes clustering nodes (Berahmand et al., 2025) and even improving GNN predictions through interpretable, optimization-based approaches (Tenorio et al., 2023; Kose et al., 2024b).

Estimating models is essential in data science, yet real-world data is known to encode historical biases that may yield unfair outcomes if incorporated in the estimation process (Chouldechova, 2017; Lambrecht and Tucker, 2019). Graph connections in particular can come with biases that are challenging to address (Lambrecht and Tucker, 2019; Yang et al., 2024). Preferences in edges between certain subpopulations have long been observed in social network analysis (Karimi et al., 2018; Stoica et al., 2018; Hofstra et al., 2017; Halberstam and Knight, 2016; Stewart et al., 2019), which can limit communication and increase disparate treatment across communities (Nilforoshan et al., 2023; Pariser, 2011; Chang et al., 2021). Even without a proclivity for linking certain groups of nodes, a poorly connected graph may yield unjust resource allocation or information spread (Ogryczak et al., 2014; Bouveret et al., 2017; Christodoulou et al., 2023).

Recovering connections from unfair data can lead to discriminatory outcomes, even if the underlying graph is not biased (Navarro et al., 2024a; Chang et al., 2021; Rahmattalabi et al., 2019). Both edges and nodal data can exhibit unfair behavior, either of which has been found to amplify harmful biases in downstream tasks (Ribeiro et al., 2023; Jiang et al., 2022). For example, a social network estimated by tracking human movement may lead to epidemic intervention strategies that discriminate across income levels (Chang et al., 2021). Unbiased graph estimation remains new and underexplored, although recent progress includes methods for particular settings (Zhou et al., 2024; Zhang and Wang, 2023; Moorthy et al., 2025; Tarzanagh et al., 2023). However, fairness has received little attention in graph signal processing (GSP) and statistics (Kose et al., 2024a; Navarro et al., 2024a,b). Indeed, the majority of work promoting fairness for graphs lies in machine learning research (Zhang et al., 2025b; Dong et al., 2023a). These approaches often require black-box tools, for which it can be challenging to develop theoretical analyses or empirical explanations to relate biases to graph data (Luo et al., 2024a). Fair models become untrustworthy if their decisions cannot be understood (Dong et al., 2022b), necessitating the use of principled approaches to mitigate biases in graphs.

We therefore propose to estimate graphs with unbiased connections from nodal observations under the assumption of *graph stationarity*. Graph stationarity can be interpreted in several equivalent ways: as data whose covariance matrix is a polynomial of the graph, as data whose covariance matrix shares the eigenvectors of the graph, or as data generated by diffusing white noise through a linear graph (network) operator (Dong et al., 2019; Mateos et al., 2019; Marques et al., 2017). Importantly, graph stationarity is a well-founded and general graph signal model that encompasses many widely used types of networked data, including Gaussian Markov random fields (GMRFs) (Marques et al., 2017). To formalize our goal of fair connectivity, we introduce two notions: *group* fairness, balancing edges across nodal groups in aggregate; and *individual* fairness, encouraging equitable links on a node-by-node basis. We then present metrics to measure biases from the two perspectives (Navarro et al., 2024a,b; Kose et al., 2024a), which we relate to the plethora of existing bias metrics. We further propose novel, alternative formulations to measure unfairness in the graph frequency domain. Equipped with these metrics, we introduce two optimization-based approaches to recover fair graphs, each founded on graph stationarity with different advantages (Segarra et al., 2017; Navarro et al., 2022). Our contributions are as follows.

- (1) We present two desirable notions of fairness on graphs from group- and node-level perspectives, or group and individual fairness, respectively, where nodes are partitioned into subpopulations based on sensitive attributes. We also explore multiple metrics to quantify graph bias, including novel formulations of bias in the graph spectrum.
- (2) We propose fair graph estimation from nodal observations through two optimization-based approaches, both founded on graph stationarity. We also demonstrate when convex relaxations of the proposed optimization problems maintain the desired solutions.
- (3) We present high-probability performance bounds in terms of both group and individual fairness, characterizing the tradeoff between fairness and accuracy in graph estimation. Importantly, we show that the fairness-accuracy tradeoff depends on the bias of the graph to be estimated, where a fair target graph can preclude a sacrifice in accuracy.

1.1 Related Work

In this section, we review past work related to fair graph estimation. This includes how past works define fairness for graphs and how these definitions are incorporated in graph machine learning and GSP.

1.1.1 GRAPH ESTIMATION

Graph estimation requires that nodal observations can be described using pairwise relationships, usually formulated through an algebraic or statistical model (Mateos et al., 2019; Dong et al., 2019). Statistical methods are among those most common, with staple models including correlation networks and GMRFs (Kolaczyk, 2009; Friedman et al., 2008; Meinshausen and Bühlmann, 2006; Buculea et al., 2025; Ying et al., 2020). Others extend the graph estimation task for specific settings such as causal relationships or particular types of dynamical processes on graphs (Rey et al., 2025; Cai et al., 2013; Baingana and Giannakis, 2017). Methods in GSP pose graph signal models to describe nodal behavior that, in some cases, generalize existing assumptions on networked data, including imposing nodal data that is smooth or low-pass on the graph (Kalofolias, 2016; Dong et al., 2016; Buculea et al.,

2022; Saboksayr and Mateos, 2021). Of particular interest to our setting are works that estimate graphs from stationary graph signals, which was originated by Segarra et al. (2017) and has been adapted for several other approaches and settings (Rey et al., 2023; Navarro et al., 2022, 2024c; Shafipour and Mateos, 2020; Pasdeloup et al., 2017). A small number of papers considered estimating graphs under considerations of fairness, which we discuss further in the sequel.

1.1.2 FAIRNESS ON GRAPHS

Past works primarily consider fairness for graphs at a node-level, analogous to traditional fairness goals. In particular, group fairness on graphs promotes balanced treatment of sub-populations of nodes (Hardt et al., 2016; Feldman et al., 2015), where it is assumed that the graph may introduce or exacerbate biased outcomes (Rahman et al., 2019; Bose and Hamilton, 2019). In such cases, graph machine learning works typically encourage group fairness for node classification or removing sensitive information from node embeddings (Ma et al., 2021; Lin et al., 2024; Palowitch and Perozzi, 2020; Kose and Shen, 2023; Dong et al., 2022a; Kose and Shen, 2022; Jiang et al., 2022; Dai and Wang, 2021). Individual fairness is a stricter definition (Dwork et al., 2012), requiring that each node be treated equitably regardless of group membership, as opposed to only balancing treatment in aggregate. However, few explicitly consider individual fairness from a graph connectivity perspective (Kose et al., 2024a; Kose and Shen, 2023), which we discuss in Section 3.2.

Alternatively, some emphasize dyadic fairness, balancing edges with respect to *pairs* of node groups, discussed in more detail in Section 3.1. A prominent application of dyadic fairness is fair link prediction, which shares our goal of promoting equity across node pairs, with applications for recommender systems (Duricic et al., 2023; Mansoury et al., 2022; Buyl and De Bie, 2020; Beutel et al., 2019), knowledge graphs (Zhang et al., 2023b; Bourli and Pitoura, 2020; Shomer et al., 2023; Fu et al., 2020), and graph transformers (Luo et al., 2024b, 2025). We next discuss obtention of fair graphs in greater detail.

1.1.3 ESTIMATING FAIR GRAPHS

Compared to machine learning, fairness for graphs in signal processing and statistics is much rarer, with few but interesting new approaches mitigating bias for graph filters (Kose et al., 2024a,b), spectral clustering (Moorthy et al., 2025; Zhang and Wang, 2023; Tarzanagh et al., 2023; Gupta and Dukkipati, 2022), and graph estimation (Navarro et al., 2024a,b; Zhou et al., 2024). Some consider estimating graphs to cluster nodes fairly (Tarzanagh et al., 2023; Zhang and Wang, 2023; Moorthy et al., 2025), but, as they are primarily interested in balancing groups across clusters, they do not explicitly encourage unbiased pairwise connections. Others promote fair connectivity by modifying edges in a given, known graph (Kose et al., 2024b; Spinelli et al., 2023; Li et al., 2021; Masrour et al., 2020; Ma et al., 2022; Agarwal et al., 2021). Additionally, fair graph generative models share our goal of creating graphs from data with unbiased edges (Wang et al., 2025; Zheng et al., 2024; Kose and Shen, 2024; Wang et al., 2023), although these require observing at least one graph to construct a distribution of similar, unbiased samples, whereas we recover graphs from observed nodal data, more relevant to certain practical applications.

The works closest to our own estimate connections from nodal data to promote fair graphs (Navarro et al., 2024a,b; Zhou et al., 2024). Navarro et al. (2024a) and Zhou et al. (2024) consider statistical approaches to estimate graphical models, although Zhou et al. (2024) assign observed samples to groups rather than nodes, which is fundamentally different from our setting. While pioneering the field of fair graph estimation, these papers consider more restrictive signal models, which are special cases of our assumption. Our work encompasses the same goal and assumptions as Navarro et al. (2024b), although we differ in our approach, implementation, and analysis. First, Navarro et al. (2024b) present similar definitions for graph fairness, albeit without much connection to past notions of bias nor our perspectives of bias in the graph spectrum. Second, we provide two new constrained optimization frameworks for estimating fair graphs from stationary graph signals. Finally, we analyze the performance of our proposed optimization problems, both in terms of accuracy and fairness, with an explicit characterization of when a tradeoff between the two can occur.

2 Preliminaries

To formalize our problem and proposed solutions, we first introduce the necessary notation and briefly review key concepts from GSP.

2.1 Notation

For any positive integer N , we let $[N] := \{1, 2, \dots, N\}$. We represent matrices and vectors by boldfaced upper-case \mathbf{X} and lower-case letters \mathbf{x} , respectively. Their entries are denoted by X_{ij} and x_i for indices i and j , and rows and columns of a matrix \mathbf{X} are denoted by $\mathbf{X}_{i,\cdot}$ and $\mathbf{X}_{\cdot,j}$, respectively. Calligraphic letters represent index sets, where $\bar{\mathcal{C}}$ denotes the complement of the index set \mathcal{C} . We let $\mathbf{X}_{\mathcal{C},\cdot}$ ($\mathbf{X}_{\cdot,\mathcal{C}}$) be the submatrix of \mathbf{X} with rows (columns) indexed by \mathcal{C} , and $\mathbf{x}_{\mathcal{C}}$ is the subvector of \mathbf{x} with entries indexed by \mathcal{C} . The boldfaced numbers $\mathbf{0}$ and $\mathbf{1}$ represent vectors of all zeros and ones, respectively, and \mathbf{I} denotes the identity matrix. We also let \mathbf{e}_i denote the i -th standard basis vector, that is, $\mathbf{e}_i := \mathbf{I}_{\cdot,i}$. For a matrix $\mathbf{X} \in \mathbb{R}^{M \times N}$, $\text{vec}(\mathbf{X}) \in \mathbb{R}^{MN}$ returns the concatenation of the columns of \mathbf{X} . We denote matrix norms by $\|\cdot\|$ and vector norms by $\|\cdot\|$, and for a matrix \mathbf{X} , $\|\mathbf{X}\|$ evaluates the vector norm of $\text{vec}(\mathbf{X})$. The operator $\text{diag}(\mathbf{X}) \in \mathbb{R}^N$ applied to a matrix returns a vector containing the diagonal entries of $\mathbf{X} \in \mathbb{R}^{N \times N}$, while $\text{diag}(\mathbf{x}) \in \mathbb{R}^{N \times N}$ returns a diagonal matrix with $\mathbf{x} \in \mathbb{R}^N$ populating the diagonal entries. We introduce two masking operators for square matrices, $\mathbf{X}^- = \text{diag}(\text{diag}(\mathbf{X}))$ retaining only diagonal entries of \mathbf{X} and $\mathbf{X}^+ = \mathbf{X} - \mathbf{X}^-$ only off-diagonal entries. We use $O(\cdot)$ for big-O notation and $o(\cdot)$ for little-o notation. The symbols \otimes , \oplus , \odot , and \circ represent the Kronecker product, the Kronecker sum, the Khatri-Rao product, and the Hadamard (element-wise) product, respectively.

2.2 Graph Signal Processing

Let $\mathcal{G} = (\mathcal{V}, \mathcal{E})$ denote a weighted, undirected graph without self-loops, consisting of N nodes collected in \mathcal{V} and edges $\mathcal{E} \subseteq \mathcal{V} \times \mathcal{V}$, where $(i, j) \in \mathcal{E}$ if and only if an edge connects nodes $i, j \in \mathcal{V}$ such that $i \neq j$. Since we are interested in recovering potentially weighted connections, we rely on the graph-shift operator (GSO) $\mathbf{S} \in \mathbb{R}^{N \times N}$ as a convenient way of

representing edges in \mathcal{G} (Sandryhaila and Moura, 2013; Djuric and Richard, 2018), where $S_{ij} \neq 0$ if and only if $(i, j) \in \mathcal{E}$. Arguably, the most common instantiations of \mathbf{S} are the adjacency matrix \mathbf{A} and the graph Laplacian $\mathbf{L} := \text{diag}(\mathbf{d}) - \mathbf{A}$ (Shuman et al., 2013; NT et al., 2021) for the node degree vector $\mathbf{d} = \mathbf{A}\mathbf{1}$, where d_i contains the sum of edge weights connected to node $i \in \mathcal{V}$. We define the set of valid adjacency matrices as

$$\mathcal{S}_A := \left\{ \mathbf{S} \in \mathbb{R}^{N \times N} \mid \mathbf{S} = \mathbf{S}^\top, \mathbf{S}^+ \geq \mathbf{0}, \text{diag}(\mathbf{S}) = \mathbf{0}, \mathbf{S}\mathbf{1} \geq \mathbf{1} \right\}. \quad (1)$$

Here, $S_{ij} \neq 0$ represents the weight of the edge (i, j) , \mathbf{S} has zero-valued diagonal entries as we consider no self-loops, and $\mathbf{S}\mathbf{1} \geq \mathbf{1}$ ensures that every node has at least one edge. We may alternatively consider $\mathbf{S} = \mathbf{L}$, which can be considered a discretization of the Laplace-Beltrami operator (Ting et al., 2010). The set of graph Laplacian matrices is defined as

$$\mathcal{S}_L := \left\{ \mathbf{S} \in \mathbb{R}^{N \times N} \mid \mathbf{S} = \mathbf{S}^\top, \mathbf{S}^+ \leq \mathbf{0}, \mathbf{S}\mathbf{1} = \mathbf{0}, \text{diag}(\mathbf{S}) \geq \mathbf{1} \right\}, \quad (2)$$

so if $\mathbf{S} \in \mathcal{S}_L$, then there exists some $\mathbf{A} \in \mathcal{S}_A$ such that $\mathbf{S} = \text{diag}(\mathbf{d}) - \mathbf{A}$, where $\mathbf{d} = \mathbf{A}\mathbf{1} = \text{diag}(\mathbf{S})$. The majority of our analyses will be demonstrated with $\mathbf{S} \in \mathcal{S}_A$ as the adjacency matrix for simplicity, but for each result we provide alternative discussions for $\mathbf{S} \in \mathcal{S}_L$ as the graph Laplacian in Appendix I. Because \mathcal{G} is undirected, \mathbf{S} can be diagonalized as $\mathbf{S} = \mathbf{V}\Lambda\mathbf{V}^\top$, where $\boldsymbol{\lambda} = \text{diag}(\boldsymbol{\Lambda})$ is the ordered vector of eigenvalues, or *graph frequencies*, of \mathbf{S} , while $\mathbf{V} = [\mathbf{v}_1, \dots, \mathbf{v}_N]$ denotes the eigenvectors of \mathbf{S} .

The field of GSP aims to process and analyze signals on graphs (Sandryhaila and Moura, 2013; Shuman et al., 2013; Djuric and Richard, 2018). We model graph signals $\mathbf{x} \in \mathbb{R}^N$ as real-valued vectors observed on \mathcal{G} , with x_i as the signal value at the i -th node. Then, we interpret the matrix-vector product $\mathbf{S}^k \mathbf{x}$ as the k -hop shift of \mathbf{x} over the graph \mathcal{G} , where the node signal x_i is propagated over the k -hop neighborhood of node i . If we collect multiple weighted shifts of graph signals, we naturally arrive at the definition of *linear graph filters* $\mathbf{H}(\mathbf{S}) = \sum_{k=0}^{\infty} h_k \mathbf{S}^k$ as polynomials of \mathbf{S} , where $\mathbf{H}(\mathbf{S})\mathbf{x}$ sums weighted diffusions of the input signal \mathbf{x} over the graph \mathcal{G} with respect to the GSO \mathbf{S} (Sandryhaila and Moura, 2013). Linear graph filtering intuitively models many real-world processes on graphs, including heat diffusion and opinion spread (Zhu et al., 2020; Thanou et al., 2017), and they form the foundation of graph convolutional networks (Gama et al., 2019).

Defining linear graph filters leads to the notion of stationary graph signals (Marques et al., 2017; Perraudeau and Vandergheynst, 2017; Girault et al., 2015). In particular, we assume our data are stationary on \mathcal{G} with respect to the GSO \mathbf{S} , where each observation can be written as an instantiation of the stochastic output of the linear graph filter $\mathbf{H}(\mathbf{S})$ excited by white input $\mathbf{w} \in \mathbb{R}^N$ such that $\mathbb{E}[\mathbf{w}] = \mathbf{0}$ and $\mathbb{E}[\mathbf{w}\mathbf{w}^\top] = \mathbf{I}$. The covariance matrix of the stationary graph signal $\mathbf{x} = \mathbf{H}(\mathbf{S})\mathbf{w}$ is $\mathbf{C} = \mathbb{E}[\mathbf{x}\mathbf{x}^\top] = \mathbf{H}(\mathbf{S})\mathbf{H}(\mathbf{S})^\top = \mathbf{H}(\mathbf{S})^2$. Thus, \mathbf{C} and \mathbf{S} share the same eigenvectors (Marques et al., 2017; Segarra et al., 2017). A critical consequence of the shared eigenbasis is that $\mathbf{C}\mathbf{S} = \mathbf{S}\mathbf{C}$, a fact commonly exploited for recovering networks from nodal data (Buciuilea et al., 2025; Shafipour and Mateos, 2020).

We are further interested in promoting fairness in graph connections, where nodes are partitioned based on sensitive information, and connections ought not to depend on the resultant subpopulations (Feldman et al., 2015; Hardt et al., 2016). In particular, each node is associated with one of G groups. For the g -th group, membership is denoted by

the indicator vector $\mathbf{z}^{(g)} \in \{0, 1\}^N$, where $z_i^{(g)} = 1$ if and only if node i belongs to group g . We collect all group labels in the indicator matrix $\mathbf{Z} = [\mathbf{z}^{(1)}, \dots, \mathbf{z}^{(G)}] \in \{0, 1\}^{N \times G}$. Groups are non-overlapping, that is, $\sum_{g=1}^G Z_{ig} = 1$ for every $i \in [N]$, where each node belongs to exactly one group. We represent the number of nodes in each group as $N_g = \sum_{i=1}^N Z_{ig}$, and because groups are non-overlapping, $N = \sum_{g=1}^G N_g$. Observe that we may collect all group sizes in the vector $\mathbf{Z}^\top \mathbf{1} = [N_1, \dots, N_G]^\top$. We let $N_{\min} = \min_g N_g$ and $N_{\max} = \max_g N_g$ denote the sizes of the smallest and largest groups, respectively. Finally, let $\mathbf{d}^{(g)} := \mathbf{d} \circ \mathbf{z}^{(g)}$ denote the masked degree vector containing only the degrees for nodes in group $g \in [G]$.

3 Measuring Bias for Graph Estimation

Our goal is to estimate the GSO \mathbf{S} of a graph such that its edges are not dependent on nodal groups. We thus formalize unbiased connectivity by presenting dyadic notions of fairness. In particular, we characterize topological bias for both group and individual fairness. Furthermore, we present a novel perspective by measuring bias in the graph frequency domain, a view that has had very limited consideration (Luo et al., 2024a,b).

3.1 Topological Group Fairness

We consider a graph with the GSO \mathbf{S} to satisfy *group fairness* if the distribution of the edge between any two nodes $i, j \in \mathcal{V}$ is independent of their groups, where we apply the definition from Navarro et al. (2024a,b); Dong et al. (2023a),

$$\mathbb{P} \left[S_{ij} \mid z_i^{(g)} = z_j^{(g')} = 1 \right] = \mathbb{P} \left[S_{ij} \mid z_i^{(h)} = z_j^{(h')} = 1 \right] \text{ for all } g, g', h, h' \in [G].$$

By the symmetry of \mathbf{S} , the following condition is equivalent

$$\mathbb{P} \left[S_{ij} \mid z_i^{(g)} = z_j^{(g)} = 1 \right] = \mathbb{P} \left[S_{ij} \mid z_i^{(g)} = z_j^{(h)} = 1 \right] \text{ for all } g, h \in [G]. \quad (3)$$

Defining topological fairness via (3) extends the notion of *demographic parity (DP)* to the dyadic setting, where DP requires that the outcome for any entity be independent of its group membership (Feldman et al., 2015). In particular, if (3) holds, then the distribution of any edge is invariant to nodal groups. Dyadic DP is the primary goal for fairness on graphs, natural for link prediction (Subramonian et al., 2024; Beutel et al., 2019) and highly relevant for social network analysis (Saxena et al., 2024; Yang et al., 2024). Many past works define fairness similarly to (3) (Yang et al., 2022; Li et al., 2021; Liu et al., 2024; Buyl and De Bie, 2021). However, most consider a weaker definition, only requiring independence for edges connecting nodes in the same group versus two different groups, which does not ensure that edge distributions are invariant to group labels; for example, under this definition we may still have $\mathbb{P}[S_{ij} \mid z_i^{(g)} = z_j^{(g)} = 1] \neq \mathbb{P}[S_{ij} \mid z_i^{(h)} = z_j^{(h)} = 1]$ for some $g \neq h$. We instead align with those that prohibit preferences toward any group pair (Pal et al., 2024; Rahman et al., 2019; Navarro et al., 2024a,b). While we consider unsigned graphs in (1) and (2), (3) does not necessitate unsigned edges (Navarro et al., 2024a; Saxena et al., 2024), whereas a large number of previous works consider not only unsigned but unweighted edges.

3.1.1 GROUP-LEVEL BIAS IN GRAPH SPATIAL DOMAIN

To assess violation of (3) in practice, we measure differences in the expected edge weights connecting nodes from each pair of groups, defining our group-wise dyadic DP metric as

$$R_G(\mathbf{S}) = \frac{1}{G^2 - G} \sum_{g \neq h} \left(\frac{\mathbf{z}^{(g)\top} \mathbf{S}^+ \mathbf{z}^{(g)}}{N_g^2 - N_g} - \frac{\mathbf{z}^{(g)\top} \mathbf{S}^+ \mathbf{z}^{(h)}}{N_g N_h} \right)^2, \quad (4)$$

where we recall that \mathbf{S}^+ is a version of \mathbf{S} with the diagonal entries set to zero. In words, $R_G(\mathbf{S})$ measures the squared difference between the average edge connecting node pairs in the same group versus in different groups, ignoring the diagonal entries.

As with our definition of group fairness in (3), similar metrics to $R_G(\mathbf{S})$ in (4) have been applied in other graph-based works to measure the violation of dyadic DP. Note that $R_G(\mathbf{S})$ was considered in (Navarro et al., 2024a), which is a modification of the group-wise metric in (Navarro et al., 2024b). In terms of dyadic fairness, $R_G(\mathbf{S})$ aligns with metrics that balance edge probabilities or link prediction scores across group pairs (Li et al., 2022; Yang et al., 2022; Liu et al., 2024; Luo et al., 2023; Khajehnejad et al., 2022). Moreover, some measures of bias in graph clustering tasks can be interpreted as quantifying topological bias (Liu et al., 2023a; Moorthy et al., 2025). Finally, while conceptually similar, some dyadic bias metrics are specific to link prediction by promoting equitable prediction accuracy, which requires known ground truth graph connectivity that we do not have for the task of graph estimation (Pal et al., 2024; Spinelli et al., 2023; Saxena et al., 2022).

3.1.2 GROUP-LEVEL BIAS IN GRAPH SPECTRAL DOMAIN

As we consider undirected edges, our GSO is diagonalizable $\mathbf{S} = \mathbf{V} \boldsymbol{\Lambda} \mathbf{V}^\top$. Therefore, we also propose to investigate bias in terms of the spectrum of \mathbf{S} , which captures relevant information about graph structure and the behavior of graph signals (Dabush and Routtenberg, 2024; NT et al., 2021). First, let $\tilde{\mathbf{z}}^{(g)} := \mathbf{V}^\top \mathbf{z}^{(g)}$ denote the *frequency response* of the group indicator vector $\mathbf{z}^{(g)}$ in terms of \mathbf{S} for every $g \in [G]$, which indicates how the g -th group is distributed throughout the graph. For example, if $\mathbf{S} \in \mathcal{S}_L$ represents the graph Laplacian and group g tends to have more *within-group connections*, then $\tilde{\mathbf{z}}^{(g)}$ has a higher concentration at *lower frequencies*. We can then equivalently express $R_G(\mathbf{S})$ from (4) as

$$\begin{aligned} R_G(\mathbf{S}) &= \frac{1}{G^2 - G} \sum_{g \neq h} \left(\frac{\mathbf{z}^{(g)\top} (\mathbf{S} - \mathbf{S}^-) \mathbf{z}^{(g)}}{N_g^2 - N_g} - \frac{\mathbf{z}^{(g)\top} \mathbf{S} \mathbf{z}^{(h)}}{N_g N_h} \right)^2 \\ &= \frac{1}{G^2 - G} \sum_{g \neq h} \left(\frac{\tilde{\mathbf{z}}^{(g)\top} \boldsymbol{\Lambda} \tilde{\mathbf{z}}^{(g)}}{N_g^2 - N_g} - \frac{\tilde{\mathbf{z}}^{(g)\top} \boldsymbol{\Lambda} \tilde{\mathbf{z}}^{(h)}}{N_g N_h} - \frac{\mathbf{z}^{(g)\top} \text{diag}(\mathbf{S})}{N_g^2 - N_g} \right)^2 \\ &= \frac{1}{G^2 - G} \sum_{g \neq h} \left[\boldsymbol{\lambda}^\top \left(\frac{\tilde{\mathbf{z}}^{(g)\top} \circ \tilde{\mathbf{z}}^{(g)}}{N_g^2 - N_g} - \frac{\tilde{\mathbf{z}}^{(g)\top} \circ \tilde{\mathbf{z}}^{(h)}}{N_g N_h} - \frac{(\mathbf{V} \circ \mathbf{V})^\top \mathbf{z}^{(g)}}{N_g^2 - N_g} \right) \right]^2. \end{aligned} \quad (5)$$

With some abuse of notation, if \mathbf{V} is known, we may write $R_G(\mathbf{S}) = R_G(\boldsymbol{\lambda})$. With (5), we can interpret how the graph frequencies $\boldsymbol{\lambda}$ and the frequency responses $\tilde{\mathbf{z}}^{(g)}$ interact to produce bias in \mathbf{S} . First, observe that if $\mathbf{S} \in \mathcal{S}_A$, then $\boldsymbol{\lambda}^\top (\mathbf{V} \circ \mathbf{V})^\top \mathbf{z}^{(g)} = \mathbf{z}^{(g)\top} \text{diag}(\mathbf{S}) = \mathbf{0}$.

In this case, for a given pair of distinct groups $g \neq h$, $R_G(\mathbf{S})$ increases with the deviation between $\tilde{\mathbf{z}}^{(g)}$ and $\tilde{\mathbf{z}}^{(h)}$, with greater effect at higher magnitudes of $\tilde{\mathbf{z}}^{(g)}$ and frequencies λ . Thus, it is more critical for groups g and h to show similar behavior at higher frequencies when $\mathbf{S} \in \mathcal{S}_A$. Second, if $\mathbf{S} \in \mathcal{S}_L$, then $\lambda^\top (\mathbf{V} \circ \mathbf{V})^\top \mathbf{z}^{(g)} = \mathbf{1}^\top \mathbf{d}^{(g)}$ sums the degrees of nodes in group g , so the difference between frequency responses $\tilde{\mathbf{z}}^{(g)}$ and $\tilde{\mathbf{z}}^{(h)}$ for $g \neq h$ must account for the differences in how well each group is connected throughout the graph. In particular, we have that $R_G(\mathbf{S}) \approx 0$ if, for all $g, h \in [G]$ such that $g \neq h$,

$$(\lambda \circ \tilde{\mathbf{z}}^{(g)})^\top \left(\frac{\tilde{\mathbf{z}}^{(g)}}{N_g^2 - N_g} - \frac{\tilde{\mathbf{z}}^{(h)}}{N_g N_h} \right) = \sum_{i=1}^N \frac{\lambda_i \tilde{z}_i^{(g)}}{N_g} \left(\frac{\tilde{z}_i^{(g)}}{N_g - 1} - \frac{\tilde{z}_i^{(h)}}{N_h} \right) \approx \frac{\mathbf{1}^\top \mathbf{d}^{(g)}}{N_g^2 - N_g}. \quad (6)$$

Observe that as $\tilde{z}_i^{(g)}$ and $\tilde{z}_i^{(h)}$ increasingly differ, particularly at high frequencies λ_i , $\mathbf{1}^\top \mathbf{d}^{(g)}$ must also increase. More intuitively, even if group g shows greater across-group connectivity than group h , we may still have $R_G(\mathbf{S}) \approx 0$ if group g is densely connected. Thus, (6) shows that differences in edge densities across groups can account for discrepancies in within-versus across-group connectivity patterns. This is expected since minimizing $R_G(\mathbf{S})$ balances the *average* edge weights across all pairs of groups. However, the left-hand side of (6) can be negative if any pair of densely connected groups differs too greatly at high frequencies, and then we cannot achieve $R_G(\mathbf{S}) \approx 0$ since the right-hand side of (6) is strictly positive.

3.2 Topological Individual Fairness

While group fairness from (3) is desirable, we may require a stricter, node-wise condition for fair connections by ensuring that each node has an equal likelihood of connecting to every group. In particular, this yields a node-wise notion of dyadic DP (Navarro et al., 2024a,b)

$$\mathbb{P} \left[S_{ij} \mid z_j^{(g)} = 1 \right] = \mathbb{P} \left[S_{ij} \mid z_j^{(h)} = 1 \right] \text{ for all } g, h \in [G], i \in [N]. \quad (7)$$

Observe that node-wise DP in (7) differs from the group-wise definition in (3) in that the condition for fair edges in (7) for a given node $i \in [N]$ does not depend on its own group. This concept is more in line with definitions of fairness that require equitable outcomes on a node-by-node basis (Rahman et al., 2019; Current et al., 2022; Chen et al., 2022; Liu et al., 2023b), also known as individual fairness (Dwork et al., 2012). However, most node-wise, individual fairness notions focus on how an external model treats or represents nodes (Dong et al., 2021; Kang et al., 2020; Sium et al., 2024; Song et al., 2022; Tsoutsouliklis et al., 2021), while our definition (7) is more related to those that consider unbiased connections (Kose et al., 2024a,b). In fact, the definition of individually fair balanced node clusters by Gupta and Dukkipati (2022) is analogous to (7) if node clusters are defined by group membership.

3.2.1 NODE-LEVEL BIAS IN GRAPH SPATIAL DOMAIN

Similarly to R_G , we consider the following node-wise DP metric for (7)

$$R_N(\mathbf{S}) = \frac{1}{GN} \sum_{g=1}^G \sum_{i=1}^N \left(\frac{[\mathbf{S}^+ \mathbf{z}^{(g)}]_i}{N_g} - \sum_{h \neq g} \frac{[\mathbf{S}^+ \mathbf{z}^{(h)}]_i}{N_h(G-1)} \right)^2, \quad (8)$$

which measures any imbalance in how each node connects across groups. To see this, observe that for terms in (8) corresponding to the i -th node, $R_N(\mathbf{S})$ sums differences in the average edge weights connecting node i to different groups. This metric serves as a measure of bias for individual fairness, where $R_N(\mathbf{S}) = 0$ only when the edge weights for each node are equally distributed across all groups. This differs from metrics that promote similar node-level treatment based on centrality or embedding similarity (Lahoti et al., 2019; Jia et al., 2024; Wang et al., 2024b). Indeed, $R_N(\mathbf{S})$ is closely related to measuring the linear correlation between group membership and neighborhoods of nodes (Kose et al., 2024a,b), which was adapted by Navarro et al. (2024b) to yield (8) to ensure that nodes do not show preferences for connecting to certain groups. Other analogous concepts balance connections at a node-by-node level, such as equitable transition probabilities across groups for random walks on graphs (Wang et al., 2023, 2024a; Arnaiz-Rodriguez et al., 2025). For example, the neighborhood fairness metric by Lee et al. (2025) measures group-wise entropy of the neighborhood of each node, indirectly encouraging more diversity in node-wise connections.

3.2.2 NODE-LEVEL BIAS IN GRAPH SPECTRAL DOMAIN

Similar to $R_G(\mathbf{S})$ in Section 3.1.2, we can express the node-wise bias $R_N(\mathbf{S})$ with respect to the spectrum of \mathbf{S} . As before, we let $\tilde{\mathbf{z}}^{(g)} = \mathbf{V}^\top \mathbf{z}^{(g)}$ be the frequency response of the group indicator vector $\mathbf{z}^{(g)}$ for each $g \in [G]$, and we write $R_N(\mathbf{S})$ from (8) as

$$\begin{aligned} R_N(\mathbf{S}) &= \frac{1}{GN(G-1)^2} \sum_{g=1}^G \left\| \mathbf{S}^+ \left[\sum_{h \neq g} \frac{\mathbf{z}^{(g)}}{N_g} - \frac{\mathbf{z}^{(h)}}{N_h} \right] \right\|_2^2 \\ &= \frac{1}{GN(G-1)^2} \sum_{g=1}^G \left\| (\mathbf{\Lambda} \mathbf{V}^\top - \mathbf{V}^\top \text{diag}((\mathbf{V} \circ \mathbf{V}) \boldsymbol{\lambda})) \left[\sum_{h \neq g} \frac{\mathbf{z}^{(g)}}{N_g} - \frac{\mathbf{z}^{(h)}}{N_h} \right] \right\|_2^2 \\ &= \frac{1}{GN(G-1)^2} \sum_{g=1}^G \left\| \sum_{h \neq g} \boldsymbol{\lambda}^\top \left[\text{diag} \left(\frac{\tilde{\mathbf{z}}^{(g)}}{N_g} - \frac{\tilde{\mathbf{z}}^{(h)}}{N_h} \right) - (\mathbf{V} \circ \mathbf{V})^\top \text{diag} \left(\frac{\mathbf{z}^{(g)}}{N_g} - \frac{\mathbf{z}^{(h)}}{N_h} \right) \mathbf{V} \right] \right\|_2^2. \end{aligned} \quad (9)$$

We again use the notation $R_N(\mathbf{S}) = R_N(\boldsymbol{\lambda})$ when the eigenvectors \mathbf{V} are known. We first observe that for $\mathbf{S} \in \mathcal{S}_A$, since $(\mathbf{V} \circ \mathbf{V}) \boldsymbol{\lambda} = \text{diag}(\mathbf{S}) = \mathbf{0}$, the bias $R_N(\mathbf{S})$ increases as the frequency response $\tilde{\mathbf{z}}^{(g)}$ differs from those of the remaining groups $\tilde{\mathbf{z}}^{(h)}$. This effect increases for higher frequencies in $\boldsymbol{\lambda}$ as for (5), but differently, $R_N(\mathbf{S})$ requires that entries of $\tilde{\mathbf{z}}^{(g)}$ and $\tilde{\mathbf{z}}^{(h)}$ exhibit similar behavior rather than only requiring similarity in aggregate. Moreover, for $\mathbf{S} \in \mathcal{S}_L$, as $(\mathbf{V} \circ \mathbf{V}) \boldsymbol{\lambda} \circ \mathbf{z}^{(g)} = \text{diag}(\mathbf{S}) \circ \mathbf{z}^{(g)} = \mathbf{d}^{(g)}$ represents group-wise node degrees, a small $R_N(\mathbf{S})$ requires that differences in frequency responses be similar to the frequency response of differences in node degrees across groups, that is, $R_N(\mathbf{S}) \approx 0$ if

$$\boldsymbol{\lambda} \circ \left(\frac{\tilde{\mathbf{z}}^{(g)}}{N_g} - \frac{\tilde{\mathbf{z}}^{(h)}}{N_h} \right) \approx \mathbf{V}^\top \left(\frac{\mathbf{d}^{(g)}}{N_g} - \frac{\mathbf{d}^{(h)}}{N_h} \right)$$

for all $g, h \in [G]$ such that $g \neq h$. Thus, differences in $\tilde{\mathbf{z}}^{(g)}$ and $\tilde{\mathbf{z}}^{(h)}$ must account for discrepancies in the distributions of connections $\mathbf{V}^\top \mathbf{d}^{(g)}$ and $\mathbf{V}^\top \mathbf{d}^{(h)}$, which aligns with our goal of balancing how edges are distributed across groups for each node.

Remark 1 The proposed metrics R_G and R_N extend classical notions of group fairness, particularly DP, to dyadic settings. Other definitions such as equalized odds (EO) or balanced performance can be similarly adapted (Li et al., 2021; Singer and Radinsky, 2022; Buyl and De Bie, 2021; Dong et al., 2023b; Liu et al., 2024; Pal et al., 2024; Saxena et al., 2022). However, these metrics require prior knowledge of graph structure, which is unlikely for inferring a network. While it is often feasible to have a limited subset of known edges, the distribution of edges across group pairs is likely to be poorly represented by this known subset, yielding an inaccurate approximation of bias. Thus, we promote DP for balancing edge connections across groups, which is known to be a prominent source of bias in GNNs and social network analysis (Saxena et al., 2024; Dong et al., 2022a). One limitation is that these dyadic extensions of DP, EO, and other definitions do not directly account for bias beyond immediate neighborhoods (Han et al., 2024; Zhang et al., 2023a; Wang et al., 2023). Since measuring the fairness of connections within a k -hop neighborhood requires powers of the GSO \mathbf{S}^k (Jalali et al., 2020), we leave this for future work.

4 Fair Network Topology Inference

Next, we consider the task of recovering an unknown graph \mathcal{G} such that our estimate has fair connections in terms of either group fairness in (3) or individual fairness in (7). To this end, we infer the GSO \mathbf{S} of \mathcal{G} from a data matrix $\mathbf{X} := [\mathbf{x}_1, \dots, \mathbf{x}_M] \in \mathbb{R}^{N \times M}$ whose columns comprise M graph signals that are stationary on \mathcal{G} with respect to \mathbf{S} . As in Section 2.2, stationarity implies that the graph signal covariance matrix \mathbf{C} and the GSO \mathbf{S} share the same eigenvectors \mathbf{V} . The eigenvectors of \mathbf{S} following the *spectral template* \mathbf{V} given by \mathbf{C} implies that $\mathbf{CS} = \mathbf{SC}$, which is a more tractable condition. Since infinitely many valid GSOs share the eigenvectors of and thus commute with \mathbf{C} (Segarra et al., 2017), we address the inference of \mathbf{S} by obtaining a target GSO with desirable structural properties (Rey et al., 2023; Zhang et al., 2025a). In particular, our goal is to obtain the sparsest GSO satisfying the conditions of graph-stationarity (Segarra et al., 2017; Marques et al., 2017), that is, we let our target GSO \mathbf{S}^* satisfy

$$\mathbf{S}^* \in \operatorname{argmin}_{\mathbf{S} \in \mathcal{S}} \|\mathbf{S}^+\|_0 \text{ s.t. } \mathbf{CS} = \mathbf{SC}, \quad (10)$$

where \mathcal{S} enforces valid GSO, such as adjacency matrices with $\mathcal{S} = \mathcal{S}_A$ in (1) or graph Laplacians with $\mathcal{S} = \mathcal{S}_L$ in (2). Because \mathbf{C} and any $\mathbf{S} \in \mathcal{S}$ are symmetric, they are both diagonalizable, so the equality constraint in (10) enforces shared eigenvectors between the target GSO \mathbf{S}^* and the covariance matrix \mathbf{C} , while the ℓ_0 (pseudo)norm encourages minimal nonzero entries in \mathbf{S}^* . We thus define our target \mathbf{S}^* as perfectly describing stationary graph signals via $\mathbf{CS}^* = \mathbf{S}^* \mathbf{C}$ while having the most parsimonious representation, allowing for interpretable analyses and reduced downstream computational complexity.

4.1 FairSpecTemp via Convex Optimization

While our goal is to obtain \mathbf{S}^* , we encounter two issues in practice: first, we typically do not have access to the true covariance matrix \mathbf{C} , and second, we require a GSO that is fair, which does not violate a level of permissible bias in our estimated graph. To address these concerns, we instead solve an approximation of the problem (10) given the sample

covariance $\hat{\mathbf{C}} := \frac{1}{M} \mathbf{X} \mathbf{X}^\top$ computed from the data matrix $\mathbf{X} \in \mathbb{R}^{N \times M}$. We present our approach *Fair Spectral Templates (FairSpecTemp)* as the following optimization problem

$$\mathbf{S}'_{\mathcal{C}} \in \operatorname{argmin}_{\mathbf{S} \in \mathcal{S}} \|\mathbf{S}^+\|_0 \text{ s.t. } \|\hat{\mathbf{C}}\mathbf{S} - \mathbf{S}\hat{\mathbf{C}}\|_F \leq \epsilon, \quad R(\mathbf{S}) \leq \tau^2. \quad (11)$$

Observe that $\tau \geq 0$ bounds the permitted structural bias measured by R , where we emphasize our proposed bias metrics $R \in \{R_G, R_N\}$; however, the constraint in (11) is adaptable to other metrics such as those in (Wang et al., 2023). Henceforth, we write R to denote either R_G or R_N , and we specify the particular metric when needed. The first constraint in (11) encourages $\mathbf{S}'_{\mathcal{C}}$ to exhibit graph stationarity given $\hat{\mathbf{C}}$ by requiring that $\mathbf{S}'_{\mathcal{C}}$ and $\hat{\mathbf{C}}$ approximately commute (Segarra et al., 2017; Navarro et al., 2022).

In practice, we instead solve a convex relaxation of (11)

$$\hat{\mathbf{S}}_{\mathcal{C}} \in \operatorname{argmin}_{\mathbf{S} \in \mathcal{S}} \|\mathbf{S}^+\|_1 \text{ s.t. } \|\hat{\mathbf{C}}\mathbf{S} - \mathbf{S}\hat{\mathbf{C}}\|_F \leq \epsilon, \quad R(\mathbf{S}) \leq \tau^2, \quad (12)$$

where (12) differs from (11) by replacing the non-convex ℓ_0 norm with a convex ℓ_1 norm. While (12) tends to be amenable to faster, simpler algorithms and yields uniqueness guarantees due to its convexity, it still involves a relaxation of (11). However, we next provide sufficient conditions under which problems (11) and (12) yield the same solution (Zhang et al., 2016; Navarro et al., 2022). To this end, we first consider vectorized versions of the constraints in problems (11) and (12). This allows us to apply guarantees for the equivalence of solutions to the problems in vectorized form (Zhang et al., 2016), thus showing that equivalent solutions exist for the original matrix-based problems (11) and (12).

First, we let \mathcal{D} , \mathcal{L} and \mathcal{U} denote index sets of diagonal, lower triangular, and upper triangular entries of any $N \times N$ matrix, that is,

$$\begin{aligned} \mathcal{D} &:= \{N(i-1) + i \mid i \in [N]\}, \\ \mathcal{L} &:= \{N(i-1) + j \mid i, j \in [N], i < j\}, \\ \mathcal{U} &:= \{N(j-1) + i \mid i, j \in [N], i < j\}. \end{aligned}$$

Then, our vector-valued optimization variable of interest is $\mathbf{s} = \operatorname{vec}(\mathbf{S})_{\mathcal{L}} \in \mathbb{R}^{N(N-1)/2}$, containing the lower triangular entries of \mathbf{S} , which completely characterizes the GSO \mathbf{S} for $\mathcal{S} \in \{\mathcal{S}_A, \mathcal{S}_L\}$. To see this, observe that since \mathbf{S} is symmetric, $\mathbf{s} = \operatorname{vec}(\mathbf{S})_{\mathcal{L}} = \operatorname{vec}(\mathbf{S})_{\mathcal{U}}$. Furthermore, if we let $\mathbf{U} := \mathbf{I}_{\mathcal{L}} + \mathbf{I}_{\mathcal{U}}$ with \mathbf{I} as the $N^2 \times N^2$ identity matrix, then $\mathbf{B}\operatorname{vec}(\mathbf{S}) = \mathbf{B}\mathbf{U}\mathbf{s}$ for any \mathbf{B} with N^2 columns. If $\mathcal{S} = \mathcal{S}_A$, $\operatorname{vec}(\mathbf{S})_{\mathcal{D}} = \mathbf{0}$, and if $\mathcal{S} = \mathcal{S}_L$, $\operatorname{vec}(\mathbf{S})_{\mathcal{D}} = -\mathbf{E}\mathbf{s}$ for $\mathbf{E} := (\mathbf{1}^\top \otimes \mathbf{I})\mathbf{U}$. Thus, we can recover any entry of \mathbf{S} from \mathbf{s} for \mathcal{S}_A or \mathcal{S}_L .

For the remainder of this section, we show our theoretical result for adjacency matrices, so we set $\mathcal{S} = \mathcal{S}_A$. However, a similar analysis for graph Laplacian GSOs, that is, $\mathcal{S} = \mathcal{S}_L$, is shown in Appendix I.1. Reminding that \oplus stands for the Kronecker sum, we define the matrix $\hat{\Sigma} := (\hat{\mathbf{C}} \oplus (-\hat{\mathbf{C}}))\mathbf{U}$, so that $\|\hat{\mathbf{C}}\mathbf{S} - \mathbf{S}\hat{\mathbf{C}}\|_F = \|\hat{\Sigma}\mathbf{s}\|_2$. We define a matrix $\mathbf{R}_G := [\check{\mathbf{r}}_G^{(1,2)}, \dots, \check{\mathbf{r}}_G^{(G-1,G)}]^\top \in \mathbb{R}^{(G^2-G) \times (N^2-N)/2}$ such that $R_G(\mathbf{S}) = \|\mathbf{R}_G\mathbf{s}\|_2^2$, where the rows of \mathbf{R}_G comprise the vectors

$$\check{\mathbf{r}}_G^{(g,h)} := \frac{1}{\sqrt{G^2 - G}} \cdot \mathbf{U}^\top \left(\frac{\mathbf{z}^{(g)} \otimes \mathbf{z}^{(g)}}{N_g^2 - N_g} - \frac{\mathbf{z}^{(g)} \otimes \mathbf{z}^{(h)}}{N_g N_h} \right) \in \mathbb{R}^{(N^2-N)/2} \quad \forall g, h \in [G], g \neq h.$$

Similarly, we define $\mathbf{R}_N := [\check{\mathbf{R}}_N^{(1)}, \dots, \check{\mathbf{R}}_N^{(G)}]^\top \in \mathbb{R}^{GN \times (N^2 - N)/2}$ such that $R_N(\mathbf{S}) = \|\mathbf{R}_N \mathbf{s}\|_2^2$ by concatenating the following G matrices

$$\check{\mathbf{R}}_N^{(g)} := \frac{1}{(G-1)\sqrt{GN}} \cdot \mathbf{U}^\top \left(\left[\sum_{h \neq g} \frac{\mathbf{z}^{(g)}}{N_g} - \frac{\mathbf{z}^{(h)}}{N_h} \right] \otimes \mathbf{I} \right) \in \mathbb{R}^{(N^2 - N)/2 \times N} \quad \forall g \in [G].$$

For $R \in \{R_G, R_N\}$, we let \mathbf{R} denote the corresponding matrix \mathbf{R}_G or \mathbf{R}_N , which we specify as needed. We next share the following result guaranteeing that a solution to the non-convex problem (11) is the unique solution to the convex problem (12).

Theorem 1 *If problems (11) and (12) are feasible for $\mathcal{S} = \mathcal{S}_A$, then for \mathbf{S}'_C as a solution to (11), we have that $\hat{\mathbf{S}}_C = \mathbf{S}'_C$ is the unique solution to (12) if*

- (i) *The submatrix $\hat{\Sigma}_{\cdot, \mathcal{I}}$ is full column rank, and*
- (ii) *There exists a constant $\psi > 0$ such that*

$$\left\| \left(\psi^{-2} \Phi^\top \Phi + \mathbf{I}_{\cdot, \bar{\mathcal{I}}} \mathbf{I}_{\bar{\mathcal{I}}, \cdot} \right)^{-1} \right\|_{\bar{\mathcal{I}}, \mathcal{I}} < 1, \quad (13)$$

where $\mathcal{I} = \text{supp}(\mathbf{s}')$ for $\mathbf{s}' = \text{vec}(\mathbf{S}'_C)_{\mathcal{L}}$, and $\Phi := [\hat{\Sigma}^\top, \mathbf{R}^\top, \mathbf{E}^\top]^\top$.

The proof is in Appendix B, which is based on that of (Segarra et al., 2017, Theorem 1) and employs (Zhang et al., 2016, Theorem 1). Condition (ii) guarantees that \mathbf{S}'_C is a solution to (12) by verifying the existence of a solution to the dual problem of (12), ensuring the existence of its associated primal solution \mathbf{S}'_C . Moreover, condition (i) guarantees that it is unique, as a full column rank $\hat{\Sigma}_{\cdot, \mathcal{I}}$ requires that there can be no other solution minimizing the ℓ_1 norm in (12). Thus, under the conditions of Theorem 1, we may solve the convex problem (12), which is also a solution to (11). As our goal is to obtain the sparsest graph satisfying the commutativity constraint, this result is theoretically satisfactory even if (11) has more than one solution. In practice, there is likely to be a single ground truth graph to be obtained, so while we can guarantee that the unique solution to (12) also minimizes the ℓ_0 norm, we cannot ensure that it approximates the ground truth GSO if (11) has more than one solution. However, we empirically find that solving a convex relaxation of (11) performs well on both synthetic and real-data simulations in Section 5. An analogous result to Theorem 1 can be found for $\mathcal{S} = \mathcal{S}_L$ in Appendix I.1.

4.2 FairSpecTemp Performance Guarantees

Our goal is to recover the target GSO \mathbf{S}^* defined in (10) by solving (11); however, under the conditions of Theorem 1, we can instead solve the convex relaxation (12) and still obtain the desired sparse estimate of \mathbf{S}^* . Thus, this section presents our main results on the performance of FairSpecTemp in terms of error bounds between the estimate $\hat{\mathbf{S}}_C$ from (12) and the target GSO \mathbf{S}^* from (10). We again restrict to adjacency matrix GSOs $\mathcal{S} = \mathcal{S}_A$, but adapting the result for graph Laplacians $\mathcal{S} = \mathcal{S}_L$ is straightforward and only changes the error bounds up to a scaling, which we explain in Appendix I.2. We require the following assumption, analogous to those considered in (Navarro et al., 2022; Segarra et al., 2017).

Assumption 1 The sample covariance matrix $\hat{\mathbf{C}} = \frac{1}{M}\mathbf{XX}^\top$ is obtained from M graph signals $\mathbf{X} = [\mathbf{x}_1, \dots, \mathbf{x}_M] \in \mathbb{R}^{N \times M}$ as diffusions of zero-mean Gaussian white noise over the graph \mathcal{G} with GSO \mathbf{S}^* , where the m -th graph signal is defined by $\mathbf{x}_m = \mathbf{H}(\mathbf{S}^*)\mathbf{w}_m$ for graph filter $\mathbf{H}(\mathbf{S}^*)$ and $\mathbf{w}_m \sim \mathcal{N}(\mathbf{0}, \mathbf{I})$. We let

- (A1) $\log N = o(M^{1/3})$,
- (A2) $\epsilon \geq c_1 N \omega \sqrt{\frac{\log N}{M}}$ for $\omega := \max\{\|\mathbf{C}^{-}\|_\infty, \|(\mathbf{S}^* \mathbf{C} \mathbf{S}^*)^{-}\|_\infty\}$ and some $c_1 > 0$,
- (A3) $\hat{\Sigma} = (\hat{\mathbf{C}} \oplus (-\hat{\mathbf{C}}))\mathbf{U}$ is full column rank with a smallest singular value $\sigma_{\min}(\hat{\Sigma}) > 0$, and
- (A4) $k \geq \sqrt{\|\text{vec}(\mathbf{S}^*)\mathcal{L}\|_0}$ for some $k \geq 0$.

We establish graph-stationarity, our setting of interest, by assuming our data are outputs of a linear graph filter applied to zero-mean white noise, as discussed in Section 2.2. The remaining items let us connect (12) to performance by ensuring a sufficiently feasible task. Assumption (A1) imposes a reasonable rate of growth of the number of samples M relative to the number of nodes N , while (A2) allows us to characterize how estimation error increases with N and decreases with M . We require (A3) to relate the minimization of the ℓ_1 norm in the objective of (12) to the commutativity constraint, which yields the bound in estimation error. Finally, observe that (A4) merely introduces a definition for the sparsity of \mathbf{S}^* , as the choice of k is arbitrary. Our first main result characterizes the performance of FairSpecTemp when considering group fairness R_G .

Theorem 2 Under Assumption 1, consider the GSO estimate $\hat{\mathbf{S}}_G \in \mathbb{R}^{N \times N}$ as the solution to (12) with the group-wise bias $R = R_G$ bounded above by $\tau \geq 0$, where group membership is encoded in the indicator matrix $\mathbf{Z} \in \{0, 1\}^{N \times G}$. Then, if the smallest group size satisfies $N_{\min} \geq 2$, the ℓ_1 error between $\hat{\mathbf{S}}_G$ and the target GSO \mathbf{S}^* in (10) is lower bounded by

$$\|\hat{\mathbf{S}}_G - \mathbf{S}^*\|_1 \geq \begin{cases} \frac{1}{2}N_{\min}\sqrt{G}(\sqrt{R_G(\mathbf{S}^*)} - \tau), & R_G(\mathbf{S}^*) > \tau^2 \\ 0, & R_G(\mathbf{S}^*) \leq \tau^2 \end{cases}, \quad (14)$$

and with probability at least $1 - e^{c_2 N}$ for some $c_2 > 0$, the error is upper bounded by

$$\|\hat{\mathbf{S}}_G - \mathbf{S}^*\|_1 \leq \begin{cases} (\phi_1 + \phi_2)\epsilon + \phi_3\sqrt{R_G(\mathbf{S}^*)}, & R_G(\mathbf{S}^*) > \tau^2 \\ \phi_1\epsilon, & R_G(\mathbf{S}^*) \leq \tau^2 \end{cases}, \quad (15)$$

$$\text{where } \phi_1 = \frac{4k(2+k)}{\sigma_{\min}(\hat{\Sigma})}, \quad \phi_2 = \frac{4(1+k)\|\mathbf{Z}^\top \mathbf{1}\|_2^2}{\sigma_{\min}(\hat{\Sigma})N_{\min}}, \quad \phi_3 = 2(1+k)G\|\mathbf{Z}^\top \mathbf{1}\|_2^2,$$

and k , $\sigma_{\min}(\hat{\Sigma})$, and ϵ are defined in Assumption 1.

The proof of Theorem 2 is in Appendix F. For the setting where \mathbf{S}^* is fair enough to be feasible, that is, $R_G(\mathbf{S}^*) \leq \tau^2$, the result follows directly from classical graph-stationary network inference (Navarro et al., 2022). Note that $N_{\min} \geq 2$ ensures that each group contains at least two nodes, as required in (4) so that balancing within- versus across-group edges is feasible.

Critically, Theorem 2 demonstrates a *conditional tradeoff between fairness and accuracy*. First, consider the case when the target GSO \mathbf{S}^* is unfair, that is, $R_G(\mathbf{S}^*) > \tau^2$. For the

upper bound between our estimate $\hat{\mathbf{S}}_C$ and \mathbf{S}^* in (15), not only will the discrepancy due to the sample covariance increase from $\phi_1\epsilon$ to $(\phi_1 + \phi_2)\epsilon$, but the bound also incurs an additional term based on the level of bias in the target $R_G(\mathbf{S}^*)$. Additionally, observe that the smallest value of $\|\mathbf{Z}^\top \mathbf{1}\|_2^2 = \sum_g N_g^2$ occurs when all groups have the same number of nodes, so the upper bound in (15) grows with the relative imbalance across groups. For the result in (14), as would be expected, an unfair \mathbf{S}^* introduces a lower bound on our estimation error, which increases as $R_G(\mathbf{S}^*)$ becomes further removed from τ^2 . Conversely, if $R_G(\mathbf{S}^*) \leq \tau^2$, then we require *no sacrifice in performance bounds* in either (14) or (15), as $\phi_1\epsilon$ corresponds to the classical error bound for estimating \mathbf{S}^* from stationary graph signals. Thus, Theorem 2 shows that if the target GSO \mathbf{S}^* is unfair, our guarantees on the performance of FairSpecTemp will necessarily suffer, but if \mathbf{S}^* is fair, then we may impose fairness for graph estimation with no consequences for our error bounds. Finally, as expected, since solving (12) yields a sparse graph, as the target \mathbf{S}^* grows denser, k increases and hence so does the upper bound $\phi_1\epsilon$.

In addition to the performance of FairSpecTemp with respect to the group-wise bias metric R_G , we also present an analogous result for individual fairness via R_N .

Theorem 3 *Under Assumption 1, consider the GSO estimate $\hat{\mathbf{S}}_C \in \mathbb{R}^{N \times N}$ as the solution to (12) with the node-wise bias $R = R_N$ bounded above by $\tau \geq 0$, where group membership is encoded in the indicator matrix $\mathbf{Z} \in \{0, 1\}^{N \times G}$. Then, the ℓ_1 error between $\hat{\mathbf{S}}_C$ and the target GSO \mathbf{S}^* in (10) is lower bounded by*

$$\|\hat{\mathbf{S}}_C - \mathbf{S}^*\|_1 \geq \begin{cases} \frac{1}{2}N_{\min}\sqrt{GN}(\sqrt{R_N(\mathbf{S}^*)} - \tau), & R_N(\mathbf{S}^*) > \tau^2 \\ 0, & R_N(\mathbf{S}^*) \leq \tau^2 \end{cases}, \quad (16)$$

and with probability at least $1 - e^{c_2 N}$ for some $c_2 > 0$, the error is upper bounded by

$$\|\hat{\mathbf{S}}_C - \mathbf{S}^*\|_1 \leq \begin{cases} (\phi_1 + \phi_4)\epsilon + \phi_5\sqrt{R_N(\mathbf{S}^*)}, & R_N(\mathbf{S}^*) > \tau^2 \\ \phi_1\epsilon, & R_N(\mathbf{S}^*) \leq \tau^2 \end{cases}, \quad (17)$$

$$\text{where } \phi_1 = \frac{4k(2+k)}{\sigma_{\min}(\hat{\Sigma})}, \quad \phi_4 = \frac{2(1+k)N_{\max}^2\sqrt{G}}{\sigma_{\min}(\hat{\Sigma})N_{\min}}, \quad \phi_5 = (1+k)N_{\max}^2\sqrt{G^3},$$

and k , $\sigma_{\min}(\hat{\Sigma})$, and ϵ are defined in Assumption 1.

The proof can be found in Appendix G, which follows similar steps to the proof of Theorem 2, excepting the steps that obtain the lower bound (16). When $R_N(\mathbf{S}^*) \leq \tau^2$ and \mathbf{S}^* is therefore feasible, the error bounds for $\hat{\mathbf{S}}_C$ are equivalent to those in (14) and (15). Theorem 3 again demonstrates a conditional tradeoff between fairness and accuracy, where an unfair \mathbf{S}^* such that $R_N(\mathbf{S}^*) > \tau^2$ increases both the upper and lower bounds on the estimation error of $\hat{\mathbf{S}}_C$, while a fair \mathbf{S}^* with $R_N(\mathbf{S}^*) \leq \tau^2$ does not negatively affect performance guarantees. Observe that the discrepancy due to imposing fairness again depends on the bias in the target GSO $R_N(\mathbf{S}^*)$, but the stricter, node-wise metric R_N has a larger lower bound in (16) than the group-wise metric R_G in (14). Moreover, the additional terms in the upper bound (17) containing ϕ_4 and ϕ_5 depend on the largest group size N_{\max}^2 , which achieves its smallest value when all groups have the same size. Theorem 3 again demonstrates that FairSpecTemp must sacrifice accuracy for fairness when the target GSO \mathbf{S}^* is biased, but a fair \mathbf{S}^* requires no tradeoff between fairness and accuracy.

Remark 2 Note that the feasibility of \mathbf{S}^* for (12) determines the upper bound for both (15) and (17) in Theorems 2 and 3, respectively. However, even if \mathbf{S}^* is not feasible, that is, $R(\mathbf{S}^*) > \tau^2$, the error bound $\phi_1\epsilon$ still holds if \mathbf{S}^* is much fairer than it is sparse. More specifically, if $R = R_G$ and $\|\mathbf{S}^*\|_1 \geq 2\|\mathbf{Z}^\top \mathbf{1}\|_2^2 \left(G\sqrt{R_G(\mathbf{S}^*)} + \frac{2\epsilon}{\sigma_{\min}(\hat{\Sigma})N_{\min}} \right)$ or if $R = R_N$ and $\|\mathbf{S}^*\|_1 \geq N_{\max}^2 \sqrt{G} \left(G\sqrt{R_N(\mathbf{S}^*)} + \frac{2\epsilon}{\sigma_{\min}(\hat{\Sigma})N_{\min}} \right)$, then the upper bound $\|\hat{\mathbf{S}}_C - \mathbf{S}^*\|_1 \leq \phi_1\epsilon$ holds with high probability. Thus, even if the target GSO \mathbf{S}^* is not fair enough to be feasible, imposing the constraint $R(\mathbf{S}^*) \leq \tau^2$ may be preferable if \mathbf{S}^* is not sparse.

Remark 3 While we bound the bias in the estimated GSO $\hat{\mathbf{S}}_C$ via τ^2 , the actual bias $R(\hat{\mathbf{S}}_C)$ may be restricted by the observed data encoded in the sample covariance matrix $\hat{\mathbf{C}}$. To see this, recall the definition of $\hat{\Sigma}$ based on $\hat{\mathbf{C}}$, and observe that under a full-column rank $\hat{\Sigma}$ as in Assumption (A3), $R(\mathbf{S}) = \|\mathbf{R}\text{vec}(\mathbf{S})_L\|_2^2 \leq \|\mathbf{R}\hat{\Sigma}^\dagger\|_2^2\epsilon^2$ for any $\mathbf{S} \in \mathcal{S}$ that may be obtained from (12). Hence, we can view $\|\mathbf{R}\hat{\Sigma}^\dagger\|_2$ as measuring the bias in the observed data, where the measurement $R(\hat{\mathbf{S}}_C)$ cannot exceed this value scaled by ϵ , which indicates that some introduced error represented by ϵ may distort the level of possible bias.

4.3 FairSpecTemp via Shared Eigenbasis

FairSpecTemp proposed in (11) encourages similar eigenvectors between $\hat{\mathbf{C}}$ and $\hat{\mathbf{S}}_C$ while directly constraining the bias in $\hat{\mathbf{S}}_C$. However, to mitigate the fairness-accuracy tradeoff shown in Theorems 2 and 3, we propose an alternative to (11) that allows us to enforce fairness implicitly. Recall that graph stationarity implies that $\mathbf{C}\mathbf{S}^* = \mathbf{S}^*\mathbf{C}$ because \mathbf{S}^* and \mathbf{C} share the same eigenvectors $\mathbf{V} = [\mathbf{v}_1, \dots, \mathbf{v}_N]$ (see Section 2.2). We can therefore equivalently define \mathbf{S}^* as

$$\mathbf{S}^*, \boldsymbol{\lambda}^* \in \underset{\mathbf{S} \in \mathcal{S}, \boldsymbol{\lambda}}{\operatorname{argmin}} \quad \|\mathbf{S}^+\|_0 \quad \text{s.t.} \quad \mathbf{S} = \sum_{i=1}^N \lambda_i \mathbf{v}_i \mathbf{v}_i^\top, \quad (18)$$

where we not only obtain the GSO \mathbf{S}^* but also its eigenvalues $\boldsymbol{\lambda}^*$ given the eigendecomposition $\mathbf{C} = \mathbf{V}\boldsymbol{\Gamma}\mathbf{V}^\top$ (Segarra et al., 2017). Since there are no conditions on $\boldsymbol{\lambda}$ in (18), the constraint $\mathbf{S} = \sum_i \lambda_i \mathbf{v}_i \mathbf{v}_i^\top$ is equivalent to the condition $\mathbf{C}\mathbf{S} = \mathbf{S}\mathbf{C}$, and therefore the sets of optimal GSOs for (18) and (10) are equivalent. We then propose an analogous approximation of (18) as in (11), where we estimate the target GSO \mathbf{S}^* given the sample covariance matrix $\hat{\mathbf{C}}$ while encouraging fair connections. With the eigendecomposition $\hat{\mathbf{C}} = \hat{\mathbf{V}}\hat{\boldsymbol{\Gamma}}\hat{\mathbf{V}}^\top$ and eigenvectors $\hat{\mathbf{V}} = [\hat{\mathbf{v}}_1, \dots, \hat{\mathbf{v}}_N]$, we propose the following adaptation of FairSpecTemp,

$$\mathbf{S}'_V, \boldsymbol{\lambda}'_V \in \underset{\mathbf{S} \in \mathcal{S}, \boldsymbol{\lambda}}{\operatorname{argmin}} \quad \|\mathbf{S}^+\|_0 \quad \text{s.t.} \quad \left\| \mathbf{S} - \sum_{i=1}^N \lambda_i \hat{\mathbf{v}}_i \hat{\mathbf{v}}_i^\top \right\|_F \leq \epsilon, \quad R(\mathbf{S}) \leq \tau^2 \quad (19)$$

for R measuring bias, where we again focus on $R \in \{R_G, R_N\}$, although this choice is flexible to other topological bias penalties (Wang et al., 2023).

Similarly to (12), we relax the ℓ_0 norm by replacing it with the convex ℓ_1 norm to get

$$\hat{\mathbf{S}}_V, \hat{\boldsymbol{\lambda}}_V \in \underset{\mathbf{S} \in \mathcal{S}, \boldsymbol{\lambda}}{\operatorname{argmin}} \quad \|\mathbf{S}^+\|_1 \quad \text{s.t.} \quad \left\| \mathbf{S} - \sum_{i=1}^N \lambda_i \hat{\mathbf{v}}_i \hat{\mathbf{v}}_i^\top \right\|_F \leq \epsilon, \quad R(\mathbf{S}) \leq \tau^2, \quad (20)$$

for which we again provide sufficient conditions under which problems (19) and (20) return the same solution. Given the definitions $\hat{\mathbf{J}} := \hat{\mathbf{V}} \odot \hat{\mathbf{V}}$ and $\hat{\mathbf{F}} = (\mathbf{I} - \hat{\mathbf{J}}\hat{\mathbf{J}}^\top)\mathbf{U}$, we present our result guaranteeing that the convex relaxation (20) is minimized by a solution to (19) as follows. As before, we show this for adjacency matrices $\mathcal{S} = \mathcal{S}_A$, but an analogous result for graph Laplacian GSOs $\mathcal{S} = \mathcal{S}_L$ can be found in Appendix I.1.

Theorem 4 *If problems (19) and (20) are feasible for $\mathcal{S} = \mathcal{S}_A$, then for \mathbf{S}'_V as a solution to (19), we have that $\hat{\mathbf{S}}_V = \mathbf{S}'_V$ is the unique solution to (20) if*

- (i) *The submatrix $\hat{\mathbf{F}}_{\cdot, \mathcal{I}}$ is full column rank, and*
- (ii) *There exists a constant $\psi > 0$ such that*

$$\left\| \left(\psi^{-2} \boldsymbol{\Psi}^\top \boldsymbol{\Psi} + \mathbf{I}_{\cdot, \bar{\mathcal{I}}} \mathbf{I}_{\bar{\mathcal{I}}, \cdot} \right)^{-1} \right\|_{\bar{\mathcal{I}}, \mathcal{I}} < 1, \quad (21)$$

where $\mathcal{I} = \text{supp}(\mathbf{s}')$ for $\mathbf{s}' = \text{vec}(\mathbf{S}'_V)_{\mathcal{L}}$, and $\boldsymbol{\Psi} := [\hat{\mathbf{F}}^\top, \mathbf{R}^\top, \mathbf{E}^\top]^\top$.

The proof of Theorem 4 is also based on (Segarra et al., 2017, Theorem 1) and (Zhang et al., 2016, Theorem 1) and shown in Appendix H. Analogously to Theorem 1, condition (ii) of Theorem 4 guarantees that \mathbf{S}'_V is a solution to (20) by verifying the existence of a solution to the dual problem of (20), while condition (i) ensures that \mathbf{S}'_V is the unique solution to (20). Under the conditions of Theorem 4, we may solve the convex problem (20) for the sparsest GSO \mathbf{S}'_V satisfying the commutativity constraint in (19) and (20).

For a final relaxation of (19), we loosen the bias constraint with respect to \mathbf{S} by solving

$$\hat{\mathbf{S}}_V, \hat{\boldsymbol{\lambda}}_V \in \underset{\mathbf{S} \in \mathcal{S}, \boldsymbol{\lambda}}{\operatorname{argmin}} \quad \|\mathbf{S}^+\|_1 \quad \text{s.t.} \quad \left\| \mathbf{S} - \sum_{i=1}^N \lambda_i \hat{\mathbf{v}}_i \hat{\mathbf{v}}_i^\top \right\|_F \leq \epsilon, \quad R(\boldsymbol{\lambda}) \leq \tau^2, \quad (22)$$

where we encourage fairness via the eigenvalues $\boldsymbol{\lambda}$ instead of the GSO \mathbf{S} . Observe that (22) estimates graphs while relaxing both the graph-stationarity and fairness constraints in comparison with (12). More specifically, jointly optimizing \mathbf{S} and $\boldsymbol{\lambda}$ allows more degrees of freedom, although this increased flexibility can cause greater error when $\hat{\mathbf{V}}$ differs further from the true eigenvectors \mathbf{V} . Moreover, by using our spectral bias metrics in (5) and (9) for (22), we promote fairness via $R(\boldsymbol{\lambda}) \approx R(\mathbf{S})$ since $\hat{\mathbf{V}}$ is known. Note that $R(\hat{\boldsymbol{\lambda}}_V) \leq \tau^2$ does not guarantee that $R(\hat{\mathbf{S}}_V) \leq \tau^2$. However, since (5) and (9) consist of terms multiplying $\boldsymbol{\lambda}$ by matrices or vectors that can be precomputed, algorithms based on (22) can enjoy far simpler computations than (20). Additionally, we show in Section 5 that, given sufficiently many samples, solving the more flexible (22) can accomplish both fair and accurate graph estimation, even when the target graph is biased.

5 Numerical Evaluation

In this section, we apply FairSpecTemp using both the commutativity condition in (12) and the shared eigenbases formulation in (22) to estimate graphs with unbiased connections, considering both group R_G and individual fairness R_N . Problems of the form in (12) or (22) are widely studied and can be solved by many efficient algorithms. We adopt the Fast

Iterative Shrinkage-Thresholding Algorithm (FISTA) to handle the associated constraints and the non-smooth ℓ_1 norm (Beck and Teboulle, 2009; Navarro et al., 2024a). To evaluate the performance of FairSpecTemp, we first conduct experiments on synthetic graphs under a variety of controlled settings. This enables us to observe situations where a trade-off between fair and accurate estimation arises, as well as others where both can be achieved simultaneously. We then move to real-world data by applying our graph estimation method to a financial investment task using historical stock market information. In this setting, the structure of the estimated graphs informs dynamic investment decisions over time.

We aim to recover a target GSO \mathbf{S}^* , which represents a ground truth graph of interest in the following simulations. To assess an estimate GSO $\hat{\mathbf{S}}$, we measure error, group-wise bias, and node-wise bias respectively as

$$d(\hat{\mathbf{S}}, \mathbf{S}^*) = \frac{\|\hat{\mathbf{S}} - \mathbf{S}^*\|_F^2}{\|\mathbf{S}^*\|_F^2}, \quad b_G(\hat{\mathbf{S}}) = \frac{(N^2 - N)\sqrt{R_G(\hat{\mathbf{S}})}}{2\|\hat{\mathbf{S}}\|_1}, \quad b_N(\hat{\mathbf{S}}) = \frac{(N^2 - N)\sqrt{R_N(\hat{\mathbf{S}})}}{2\|\hat{\mathbf{S}}\|_1}, \quad (23)$$

where the bias is normalized by average edge weight. Throughout the ensuing simulations, we consider the following methods: (i) **ST**: SpecTemp without fairness, that is, (12) with $\tau = \infty$ (Segarra et al., 2017); (ii) **FST_C-R_G**: FairSpecTemp via (12) with $R = R_G$; (iii) **FST_C-R_N**: FairSpecTemp via (12) with $R = R_N$; (iv) **FST_V-R_G**: FairSpecTemp via (22) with $R = R_G$; (v) **FST_V-R_N**: FairSpecTemp via (22) with $R = R_N$; (vi) **ST-Rw**: SpecTemp with randomly rewired edges; (vii) **ST-Ba**: SpecTemp with edges reweighted to be balanced across group pairs; and (viii) **FGL**: Fair GLASSO (Navarro et al., 2024a), estimating fair Gaussian graphical models with $R = R_G$. As discussed in Section 1.1, fair graph estimation from nodal data is highly limited, with **FGL** as one existing method developed for the same task, albeit assuming a stricter graph signal model. Hence, we consider additional baselines to evaluate how well FairSpecTemp can recover fair, accurate graphs. In particular, for **ST-Rw**, we randomly rewire edges of the **ST** estimate, which, with sufficiently many rewirings, effectively decouples dependencies between edges and group labels. However, rewiring edges may not reduce bias for highly imbalanced groups since edge densities across group pairs may be relatively unchanged. We therefore also consider **ST-Ba**, where we maintain the support of the initial **ST** estimate and instead rescale GSO entries for more balanced edge weights across pairs of groups. The code to reproduce all results, along with implementation details, is available on GitHub¹.

5.1 Group Versus Individual Fairness

We first estimate unbiased graphs by imposing either group fairness via R_G in (4) or individual fairness via R_N in (8) as the connectivity of the target graph \mathbf{S}^* varies. We compare **ST** to all four variants of FairSpecTemp, (12) and (22) with $R \in \{R_G, R_N\}$. We consider $N = 40$ nodes, $G = 2$ groups, $M = 10^5$ graph signals, and, for a fixed number of edges, we modify the topology in \mathbf{S}^* to vary the bias $R_G(\mathbf{S}^*)$ or $R_N(\mathbf{S}^*)$. In particular, we examine the following two scenarios.

First, we vary the ratio of across-group edges, altering both $R_G(\mathbf{S}^*)$ and $R_N(\mathbf{S}^*)$. We start with a graph that is highly modular with respect to groups, where the fraction of

1. https://github.com/mn51/fair_nti

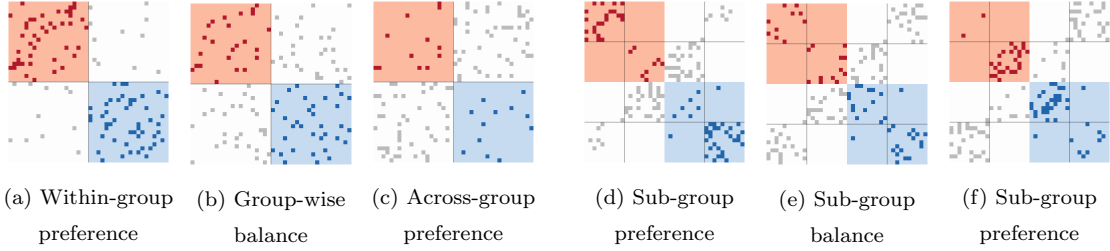


Figure 1: Target \mathbf{S}^* as $R_G(\mathbf{S}^*)$ and $R_N(\mathbf{S}^*)$ vary. Red denotes node pairs in group 1, blue node pairs in group 2, and gray node pairs in different groups. Both $R_G(\mathbf{S}^*)$ and $R_N(\mathbf{S}^*)$ vary in (a)-(c), while $R_G(\mathbf{S}^*)$ is low but $R_N(\mathbf{S}^*)$ varies in (d)-(f). (a) Majority of edges connect the *same* group ($R_G(\mathbf{S}^*)$ and $R_N(\mathbf{S}^*)$ high). (b) Balanced number of edges within and across groups ($R_G(\mathbf{S}^*)$ and $R_N(\mathbf{S}^*)$ low). (c) Majority of edges connect *different* groups ($R_G(\mathbf{S}^*)$ and $R_N(\mathbf{S}^*)$ high). (d) Subgroups of nodes show strong within- or across-group preferences ($R_G(\mathbf{S}^*)$ low, $R_N(\mathbf{S}^*)$ high). (e) Every node has relatively balanced edges across groups ($R_G(\mathbf{S}^*)$ and $R_N(\mathbf{S}^*)$ low). (f) Alternate subgroups of nodes show strong within- or across-group preferences ($R_G(\mathbf{S}^*)$ low, $R_N(\mathbf{S}^*)$ high).

across-group edges is 0.2, visualized in Figure 1(a). Then, we randomly rewire an increasing number of within-group edges to connect nodes across groups until the across-group fraction is 0.8, that is, the graph is highly bipartite with respect to groups, shown in Figure 1(c). The graph is fair with respect to both $R_G(\mathbf{S}^*)$ and $R_N(\mathbf{S}^*)$ when the across-group edge ratio is 0.5 in Figure 1(b), as each node has an equal likelihood of connecting to either group. We plot the error, group-wise bias, and node-wise bias for the estimated GSOs in Figure 2(a)-(c) corresponding to the scenario in Figure 1(a)-(c). As expected, all FairSpecTemp approaches achieve fairer GSOs than **ST**. However, when \mathbf{S}^* is unfair, that is, the across-group edge ratio is closer to 0 or 1, the improved bias comes at a sacrifice in accuracy, particularly for **FST_C-R_G** and **FST_V-R_G**, which yield the lowest group-wise bias b_G . Conversely, when \mathbf{S}^* is fair with an across-group edge ratio of 0.5, only **FST_C-R_G** and **FST_V-R_G** rival **ST** in both error and group-wise bias b_G . Interestingly, **FST_V-R_G** also improves the node-wise bias b_N , aligning with our intuition that the increased degrees of freedom for (22) allows greater flexibility in estimation, potentially mitigating the tradeoff between fairness and accuracy.

Second, we consider a low $R_G(\mathbf{S}^*)$ but a varying $R_N(\mathbf{S}^*)$. To this end, we partition both groups into two subgroups. We first generate a graph such that one subgroup per group exhibits high within-group connectivity, and we randomly rewire an increasing subset of these edges to connect across groups. Similarly, the remaining two subgroups exhibit high across-group connectivity, which are increasingly rewired to become within-group edges. Since the number of within- versus across-group edges remain balanced, the group-wise bias $R_G(\mathbf{S}^*)$ remains low, but if the fraction of rewired edges is close to 0 or 1 as depicted in Figure 1(d) and (f), then $R_N(\mathbf{S}^*)$ will be high, as nodes show strong preferences for either within- or across-group connections. Figure 1(e) shows when $R_N(\mathbf{S}^*)$ is low, that is, when the fraction of rewired edges is 0.5, as all nodes demonstrate balanced connectivity between both groups. Graph estimation performance for this setting is shown in Figure 2(d)-(f).

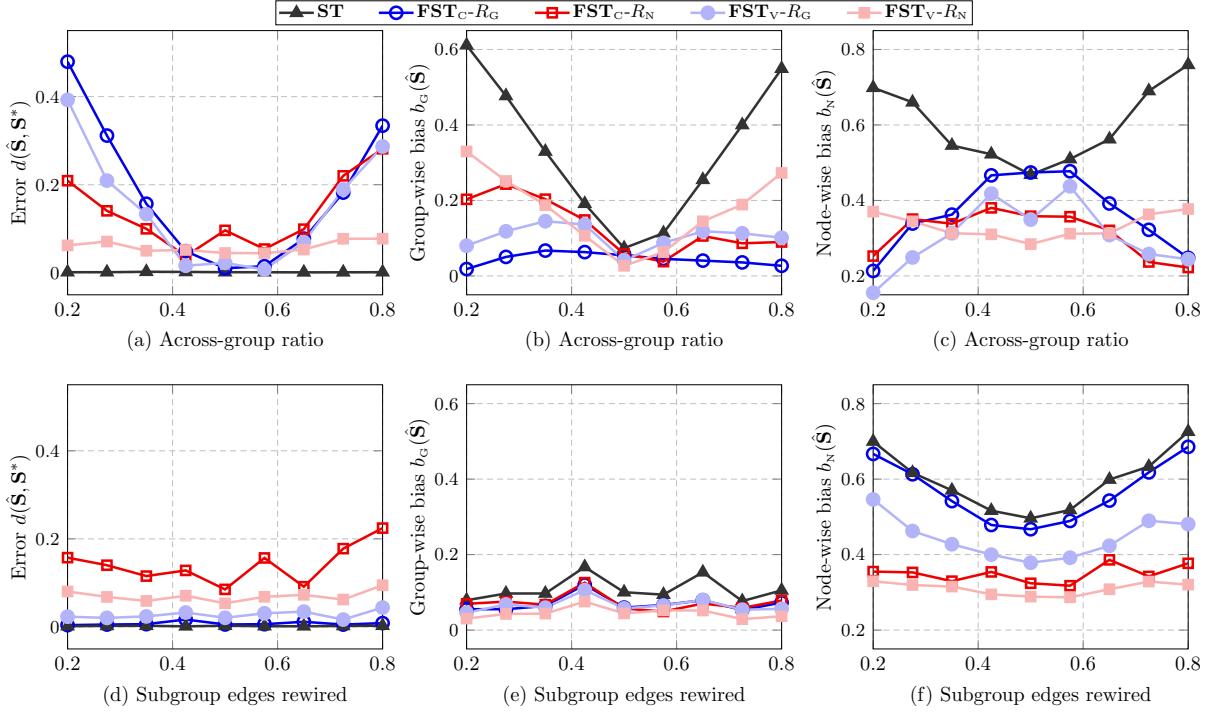


Figure 2: **Top row:** Performance of estimates $\hat{\mathbf{S}}$ as $R_G(\mathbf{S}^*)$ and $R_N(\mathbf{S}^*)$ vary corresponding to Figure 1(a)-(c). **Bottom row:** Performance of estimates $\hat{\mathbf{S}}$ for low $R_G(\mathbf{S}^*)$ as $R_N(\mathbf{S}^*)$ varies corresponding to Figure 1(d)-(f). **Left column:** (a) and (d) depict estimation error $d(\hat{\mathbf{S}}, \mathbf{S}^*)$. **Middle column:** (b) and (e) show group-wise bias $b_G(\hat{\mathbf{S}})$. **Right column:** (c) and (f) show node-wise bias $b_N(\hat{\mathbf{S}})$.

Since $R_G(\mathbf{S}^*)$ is always low, the group-wise fair methods **FST_C-R_G** and **FST_V-R_G** obtain estimates similarly as accurate as **ST**, and all methods obtain a low group-wise bias b_G . However, only **FST_C-R_N** and **FST_V-R_N** also reduce the node-wise bias b_N , with the greatest sacrifice in accuracy for **FST_C-R_N**. Indeed, Figure 2 demonstrates scenarios where (22) exhibits superior performance, as **FST_V-R_N** shows the lowest bias in terms of both b_G and b_N with less error than **FST_C-R_N**, while **FST_V-R_G** may incur greater b_N , yet it remains lower than that of **FST_C-R_G**. Figure 2 illustrates scenarios in which we may prefer encouraging group versus individual fairness by choice of R ; in the remaining experiments, we focus on the more common goal of group fairness, that is, we measure estimation bias with b_G .

5.2 Performance as Graph Size Varies

To further investigate the differences between FairSpecTemp in (12) and (22), we next consider estimating unbiased graphs as the number of nodes increases. We generate Erdos-Renyi (ER) graphs with $G = 2$ groups and $M = 10^6$ stationary graph signals while increasing the number of nodes N . To maintain comparable sparsity as N varies, we let the ER edge probabilities be $p = \frac{5}{N-1}$ for a constant expected degree of 5. We compare

graph estimation with and without the fairness constraints: **ST**, **FST**_C- R_G , and **FST**_V- R_G . Figure 3(a) reports both the estimation error $d(\hat{\mathbf{S}}, \mathbf{S}^*)$ (left y -axis) and the group-wise bias $b_G(\hat{\mathbf{S}})$ (right y -axis). As expected, both FairSpecTemp approaches achieve lower bias than **ST**, but **FST**_C- R_G with an explicit bias constraint $R_G(\hat{\mathbf{S}}) \leq \tau^2$ exhibits more stability in both bias and error across all graph sizes N . In contrast, **FST**_V- R_G maintains a higher error than both **FST**_C- R_G and **ST**, yet only **FST**_V- R_G decreases both error and bias as N increases, with a more competitive error between **FST**_V- R_G and **FST**_C- R_G at $N = 100$. Thus, while **FST**_C- R_G produces the more expected result of balancing bias and error, the more flexible **FST**_V- R_G can obtain fairer graphs for larger graph sizes.

5.3 Estimating Fair Graphs from Biased Data

We next consider a setting likely to be encountered in real-world data: The graph structure to be estimated is fair, but the observed data is biased. To simulate an increasing level of within-group preference in the graph data, we first generate an ER graph with GSO \mathbf{S}^* of $N = 100$ nodes and edge probability $p = 0.05$ so the connections are fair with respect to the $G = 2$ nodal groups. Then, we progressively bias the connections in \mathbf{S}^* by increasing within-group edge weights while simultaneously decreasing across-group edge weights, and we generate increasingly biased sets of $M = 10^6$ samples from the perturbed graphs. We plot the error and group-wise bias for the estimated graphs in Figure 3 as the level of bias in the data increases. Each curve corresponds to a method **ST**, **ST-Ba**, **FST**_C- R_G , **FST**_V- R_G , and **FST**_C- R_N , and filled, darker markers represent the least biased data.

We observe that **ST** sees the greatest degradation in terms of both accuracy and fairness, whereas all FairSpecTemp methods become less accurate as the data grows more biased but maintain lower bias in estimation. Since we inject bias in data via imbalanced edge weights, we examine how effectively **ST-Ba** can mitigate this effect by rebalancing edge weights. As expected, reweighting edges in **ST-Ba** may reduce bias, but altering the estimate from **ST** can require a larger sacrifice of accuracy for a sufficiently fair outcome. As for the node-wise **FST**_C- R_N , we consistently see slightly higher bias and error relative to both **FST**_C- R_G and **FST**_V- R_G . This is particularly noticeable when the bias in the data is small (filled markers in Figure 3(b)), as the stricter node-wise constraint for **FST**_C- R_N may struggle to achieve a similarly low bias without a greater sacrifice in accuracy, as shown in Figure 2. We also note a tradeoff between **FST**_C- R_G and **FST**_V- R_G as the observed data differs further from the true, fair distribution. When the data is fairer, both **FST**_C- R_G and **FST**_V- R_G achieve Pareto optimal solutions with comparable fairness and accuracy. However, as the bias in the data grows, **FST**_V- R_G maintains the fairest estimates but incurs increasingly greater error, whereas graphs estimated via **FST**_C- R_G may not be as fair, but in comparison with **ST**, **FST**_C- R_G maintains a competitive accuracy with far lower bias.

5.4 Comparing Fair Graph Estimation Approaches

We compare FairSpecTemp in (12) and (22) with different fair graph estimation baselines, where we estimate ER graphs of $N = 100$ nodes and an edge probability $p = 0.05$ for $G = 2$ imbalanced groups. We show bias and error as the number of stationary graph signals increases from $M = 10^2$ (filled markers) to $M = 10^6$ in Figure 3(c). Since the true graph \mathbf{S}^* is biased due to imbalanced groups, a consistent trend across methods is an increase

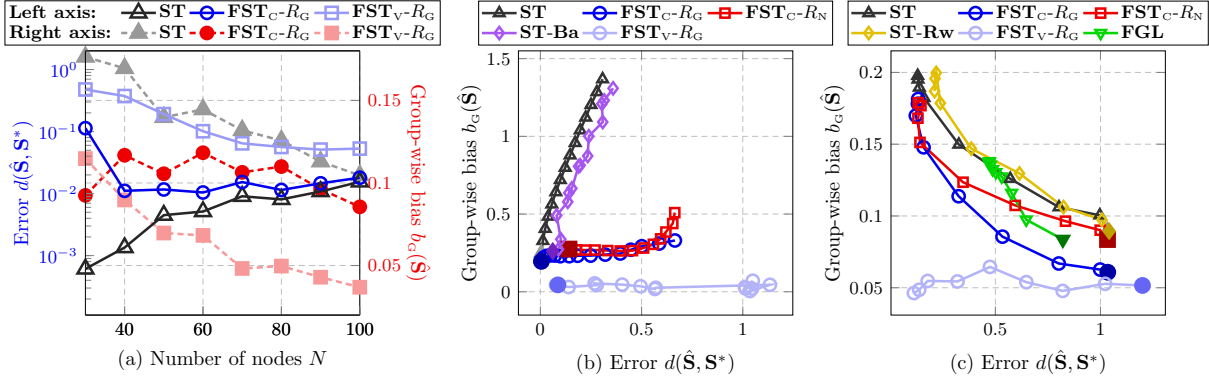


Figure 3: Performance of estimates $\hat{\mathbf{S}}$ for different graph estimation methods under varying conditions. Bias $b_G(\hat{\mathbf{S}})$ and error $d(\hat{\mathbf{S}}, \mathbf{S}^*)$ (a) as the number of nodes N increases, (b) as the data becomes more biased toward within-group connections, (c) as the number of samples M increases.

in both accuracy and group-wise bias as M increases. In general, all fair graph methods achieve lower bias than **ST** for all values of M . The random edge rewirings in **ST-Rw** can achieve slight improvements in bias relative to **ST**, but the additional stochasticity also introduces a slight increase in error. While **FGL** obtains consistently fairer graphs than **ST**, it assumes a stricter signal model than our graph-stationarity assumption, yielding worse error at higher M . As for FairSpecTemp methods, we first note the value of direct bias constraints via (12): **FST_C-R_G** and **FST_C-R_N** both achieve lower bias than **ST** while maintaining accuracy. However, since R_N is stricter than R_G , **FST_C-R_N** requires a looser constraint to maintain competitive accuracy, hence the fairer estimates from **FST_C-R_G**. We also observe the different advantages between FairSpecTemp in (12) and (22). When M is low, our estimates of the covariance matrix eigenvectors $\hat{\mathbf{V}}$ will be poor and therefore detrimental for the flexible **FST_V-R_G**, therefore applying **FST_C-R_G** is preferable. However, in a high-sample regime, we observe the power of increased degrees of freedom in **FST_V-R_G**, as we achieve competitive accuracy in estimation, but we see a dramatic improvement in bias for **FST_V-R_G** relative to all other methods. This reveals the value of both variants of FairSpecTemp. We may require explicit bias constraints via **FST_C-R_G**, but certain settings allow us to mitigate the tradeoff between fairness and accuracy using **FST_V-R_G**.

5.5 Estimating Fair Graphs for Investing

Finally, we apply graph estimation and our group-wise bias metric R_G for a real-world financial investment task, where we estimate graphs from real-world market data. Specifically, we consider graphs connecting companies from the S&P 500 index with groups corresponding to different sectors, and, as our nodal observations, we observe company log-returns indicating changes in market value over time. A given set of N companies and M daily log-return values comprises a data matrix $\mathbf{X} \in \mathbb{R}^{N \times M}$ from which we estimate graphs indicating which companies exhibit similarities in their return profiles. Thus, a common

approach is to use graph structure to design investment strategies, such as investing when the graph exhibits low connectivity since minimizing correlations among investments is key to reducing risk (Cardoso and Palomar, 2020). We instead consider employing $b_G(\hat{\mathbf{S}})$ by investing when the *group-wise bias* is sufficiently high. Indeed, since companies typically exhibit more similar behavior within the same sector, we may expect a higher $b_G(\hat{\mathbf{S}})$ in general due to within-group edge preferences. Thus, a low $b_G(\hat{\mathbf{S}})$ implies a notable increase in similarities across sectors, indicating a riskier period such as the COVID-19 pandemic. We proceed with financial investment in two scenarios, one short-term with frequent investments opportunities and another, longer-term setting with less frequent graph evaluations.

The first setup involves a three-month window in which we estimate a graph $\hat{\mathbf{S}}_t$ every other day via sliding windows of log-return observations from February 2020 to May 2020, where the $N = 71$ nodes represent companies from $G = 3$ sectors: Communication Services, Materials, and Energy, chosen for their relative balance in group size. We obtain a sequence of graphs $\{\hat{\mathbf{S}}_t\}_{t=1}^{38}$, from which we estimate the time-varying group-wise bias $\{b_G(\hat{\mathbf{S}}_t)\}_{t=1}^{38}$. If the bias exceeds a threshold, then this implies greater diversity across sectors and we invest; otherwise, we do not. Figure 4(a) shows the value of investment for different graph estimation approaches and the group-wise bias of the estimated graphs. We compare **ST**, **ST-Rw**, **FST_C-R_G**, and **FST_C-R_N**, along with two more traditional approaches, one estimating a correlation matrix across companies, referred to as **Corr.**, and the baseline **Strategy I**, which refers to investing and selling every other day, regardless of bias $b_G(\hat{\mathbf{S}}_t)$ (Cardoso and Palomar, 2020). For a fair comparison, each method is assigned the threshold that yields the largest possible final investment value. Figure 4(a) illustrates that **FST_C-R_G** clearly outperforms its competitors with the highest value at the end of the investment period, with **FST_C-R_N** and **ST** as the next best. A closer look at the bias in Figure 4(a) shows that **FST_C-R_G**, **FST_C-R_N**, and **ST** show similar trends of lower values of $b_G(\hat{\mathbf{S}}_t)$ around March 2020, the period in which investment was unwise based on the steep decrease in value of the naive **Strategy I**. However, since **ST** and **FST_C-R_N** do not explicitly encourage low group-wise bias, they experience greater noise in $b_G(\hat{\mathbf{S}}_t)$ over time, which can yield false positive investment flags. In contrast, **FST_C-R_G** returns a consistently more stable sequence $b_G(\hat{\mathbf{S}}_t)$, so higher values of bias are more indicative of appropriate investment opportunities.

For the second setup, we consider a more challenging scenario with a longer period, from January 2019 to December 2022; less frequent investment opportunities, estimating graphs weekly for graph sequences of length 170; and a larger number of companies $N = 112$ spanning a different set of sectors: Real Estate, Energy, and Healthcare. We again present the investment value and estimated bias $b_G(\hat{\mathbf{S}})$ in Figure 4(b), which support our observations from the short-term setup in Figure 4(a). Prior to the COVID-19 pandemic, all methods behave similarly; however, starting early 2020, only **ST**, **FST_C-R_G**, and **FST_C-R_N** both maintain and increase their value in comparison with **ST-Rw**, **Corr.**, and **Strategy I**, which experience a large decrease in value at the beginning of the pandemic. Here, **FST_C-R_N** obtains the highest return value, closely followed by **FST_C-R_G** and **ST**. In such a setting with more companies and larger gaps in between investment opportunities, we find a potential advantage to imposing node-wise fairness by specifically encouraging each node show diversity in similarity across sectors. This more explicit encouragement of diversity in connectivity may be necessary for larger-scale, volatile situations. Thus, we not only demonstrate the value of our bias metrics for real-world applications, where we impose

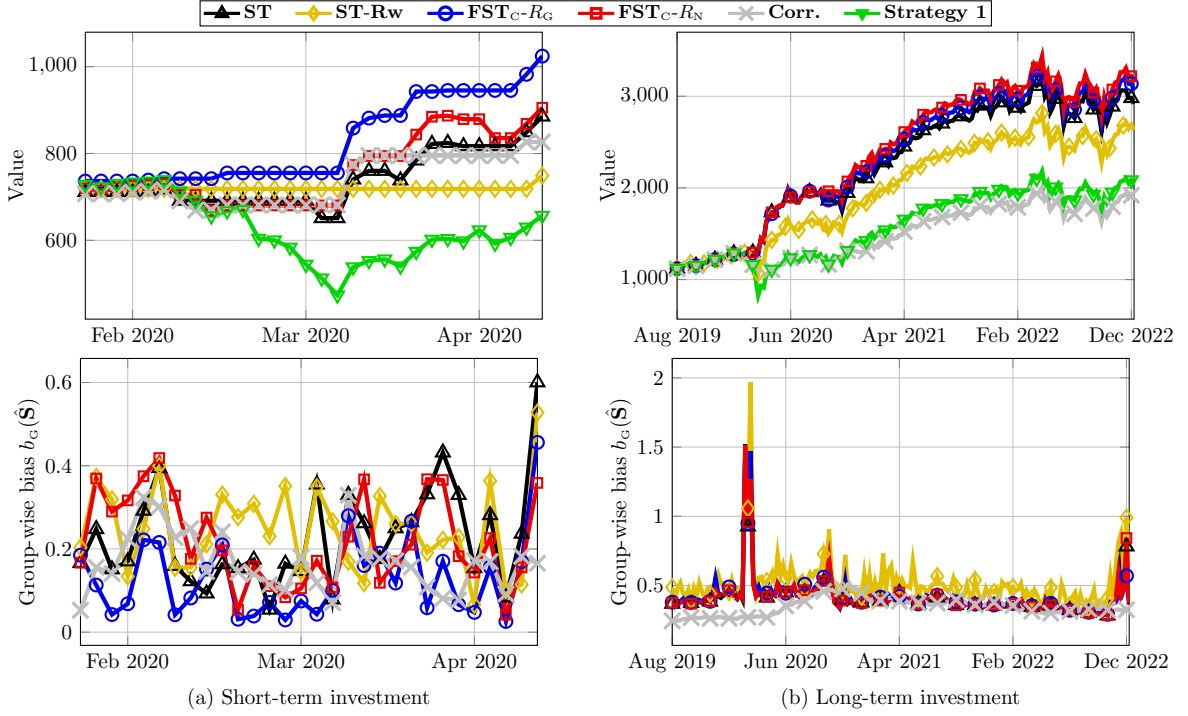


Figure 4: Investment value and group-wise bias $b_G(\hat{S})$ of estimated graphs \hat{S} over time: (a) three months estimating graphs every other day and (b) two years and five months with weekly graph estimation.

more informative structural rules for investment that lead to reliable strategies, but we also show that FairSpecTemp performs well with our proposed investment strategy.

6 Conclusion

In this work, we defined group and individual fairness for graphs, along with metrics to quantify topological bias. These metrics allowed us to propose two constrained optimization problems for estimating fair graphs from stationary graph signals, with performance guarantees demonstrating when we do or do not experience a tradeoff between fairness and accuracy. Future work will see expansion towards other definitions of fairness for graph connectivity, such as extending the notions of multi-precision to graphs. As mentioned previously, most existing topological bias metrics consider fairness in terms of single-hop connections, but we aim to develop similar, effective approaches with multi-hop fairness considerations. Moreover, we may estimate fair graphs while determining the optimal balance between group or individual fairness, which we can impose through adaptive or bilevel optimization. We also plan to extend this task to more difficult graph settings such as estimating unbiased directed graphs for fair influence maximization. As another example, nodes in social networks often do not have known group memberships. Finally, our optimization-based, GSP-driven work aims to participate in the push towards the inter-

section between GSP and graph-based machine learning. Incorporating well-founded tools into highly effective models leads to trustworthy yet powerful methods, a necessity for tools increasingly being employed in large-scale yet sensitive applications.

Acknowledgments and Disclosure of Funding

Research was supported by NSF under award CCF-2340481, the Army Research Office under Grant Number W911NF-17-S-0002, the Spanish AEI (10.13039/501100011033) grants PID2022-136887NB-I00 and PID2023-149457OB-I00, and the Community of Madrid via the Ellis Madrid Unit and grants URJC/CAM F1180 and TEC-2024/COM-89. The views and conclusions contained in this document are those of the authors and should not be interpreted as representing the official policies, either expressed or implied, of the Army Research Office or the U.S. Army or the U.S. Government. The U.S. Government is authorized to reproduce and distribute reprints for Government purposes notwithstanding any copyright notation herein.

Appendix A. Auxiliary Results

Lemma 1 (Claim 2, Navarro et al. 2022) *Under conditions (A1) and (A2) of Assumption 1, with probability at least $1 - e^{-c_2 \log N}$ for some constant $c_2 > 0$, we have that*

$$\|\hat{\mathbf{C}}\mathbf{S}^* - \mathbf{S}^*\hat{\mathbf{C}}\|_F \leq \epsilon. \quad (24)$$

Lemma 2 *For any $\mathbf{s} \in \mathbb{R}^{\frac{1}{2}(N^2-N)}$ such that $\mathbf{s} \geq \mathbf{0}$, $\|\hat{\Sigma}\mathbf{s}\|_2 \leq \epsilon$, and $\|\mathbf{R}_G\mathbf{s}\|_2 \leq \tau < \|\mathbf{R}_G\mathbf{s}^*\|_2$,*

$$\|\mathbf{s}\|_1 \leq \|\mathbf{Z}^\top \mathbf{1}\|_2^2 \left(G\|\mathbf{R}_G\mathbf{s}^*\|_2 + \frac{2\epsilon}{\sigma_{\min}(\hat{\Sigma})N_{\min}} \right). \quad (25)$$

Lemma 3 *For any $\mathbf{s} \in \mathbb{R}^{\frac{1}{2}(N^2-N)}$ such that $\mathbf{s} \geq \mathbf{0}$, $\|\hat{\Sigma}\mathbf{s}\|_2 \leq \epsilon$, and $\|\mathbf{R}_N\mathbf{s}\|_2 \leq \tau < \|\mathbf{R}_N\mathbf{s}^*\|_2$,*

$$\|\mathbf{s}\|_1 \leq \frac{N_{\max}^2 \sqrt{G}}{2} \left(G\|\mathbf{R}_N\mathbf{s}^*\|_2 + \frac{2\epsilon}{\sigma_{\min}(\hat{\Sigma})N_{\min}} \right). \quad (26)$$

Appendix B. Proof of Theorem 1

Let \mathbf{R} denote the matrix \mathbf{R}_G or \mathbf{R}_N corresponding to the choice of R . We introduce the following vectorization of the optimization problem (11) as

$$\mathbf{s}' \in \operatorname{argmin}_{\mathbf{s}} \|\mathbf{s}\|_0 \quad \text{s.t.} \quad \|\hat{\Sigma}\mathbf{s}\|_2 \leq \epsilon, \quad \|\mathbf{R}\mathbf{s}\|_2 \leq \tau, \quad \mathbf{E}\mathbf{s} \geq \mathbf{1}, \quad \mathbf{s} \geq \mathbf{0}, \quad (27)$$

where $\mathbf{s}' = \operatorname{vec}(\mathbf{S}'_{\mathcal{L}})$. We also vectorize the problem (12) as

$$\hat{\Omega} = \operatorname{argmin}_{\mathbf{s}} \|\mathbf{s}\|_1 \quad \text{s.t.} \quad \|\hat{\Sigma}\mathbf{s}\|_2 \leq \epsilon, \quad \|\mathbf{R}\mathbf{s}\|_2 \leq \tau, \quad \mathbf{E}\mathbf{s} \geq \mathbf{1}, \quad \mathbf{s} \geq \mathbf{0}. \quad (28)$$

We proceed with showing that under the conditions of Theorem 1, the solution set $\hat{\Omega}$ is a singleton containing only \mathbf{s}' . Recall that $\Phi = [\hat{\Sigma}^\top, \mathbf{R}^\top, \mathbf{E}^\top]^\top$, and consider the auxiliary problem for a given solution $\hat{\mathbf{s}} \in \hat{\Omega}$

$$\tilde{\Omega}(\hat{\mathbf{s}}) = \operatorname{argmin}_{\mathbf{s}} \|\mathbf{s}\|_1 \text{ s.t. } \Phi \mathbf{s} = \Phi \hat{\mathbf{s}}. \quad (29)$$

Observe that any solution in $\tilde{\Omega}(\hat{\mathbf{s}})$ is non-negative, thus we need only consider the first three constraints of (28). To see this, let $\tilde{\mathbf{s}} \in \tilde{\Omega}(\hat{\mathbf{s}})$.

$$\|\tilde{\mathbf{s}}\|_1 \leq \|\hat{\mathbf{s}}\|_1 = \mathbf{1}^\top \mathbf{E} \hat{\mathbf{s}} = \mathbf{1}^\top \mathbf{E} \tilde{\mathbf{s}} \leq \|\tilde{\mathbf{s}}\|_1,$$

thus $\|\tilde{\mathbf{s}}\|_1 = \mathbf{1}^\top \tilde{\mathbf{s}}$ and so $\tilde{\mathbf{s}} \geq \mathbf{0}$. Moreover, we have that $\hat{\mathbf{s}} \in \tilde{\Omega}(\hat{\mathbf{s}})$. We proceed with showing that \mathbf{s}' is the unique solution to (29), that is, $\tilde{\Omega}(\hat{\mathbf{s}}) = \{\mathbf{s}'\}$.

If there exists a vector \mathbf{y} such that $\mathbf{y} \in \operatorname{Im}(\Phi^\top)$, $\mathbf{y}_{\mathcal{I}} = \operatorname{sign}(\mathbf{s}'_{\mathcal{I}})$, and $\|\mathbf{y}_{\bar{\mathcal{I}}}\|_\infty < 1$, then $\mathbf{s}' \in \tilde{\Omega}(\hat{\mathbf{s}})$ (Zhang et al., 2016). Thus, consider the following optimization problem

$$\min_{\mathbf{y}_{\bar{\mathcal{I}}}, \mathbf{r}} \|\mathbf{y}_{\bar{\mathcal{I}}}\|_2^2 + \psi^2 \|\mathbf{r}\|_2^2 \quad \text{s.t.} \quad \mathbf{y}_{\bar{\mathcal{I}}} = \Phi_{\cdot, \bar{\mathcal{I}}}^\top \mathbf{r}, \quad \Phi_{\cdot, \mathcal{I}}^\top \mathbf{r} = \operatorname{sign}(\mathbf{s}'_{\mathcal{I}}).$$

Then, with $\mathbf{t} = [\psi \mathbf{r}^\top, -\mathbf{y}_{\bar{\mathcal{I}}}^\top]^\top$ and $\mathbf{Q} = [\psi^{-1} \Phi^\top, \mathbf{I}_{\cdot, \bar{\mathcal{I}}}]$, we can rewrite the above problem as

$$\min_{\mathbf{t}} \|\mathbf{t}\|_2^2 \quad \text{s.t.} \quad \mathbf{Q} \mathbf{t} = \mathbf{I}_{\cdot, \mathcal{I}} \operatorname{sign}(\mathbf{s}'_{\mathcal{I}}),$$

which has solution $\mathbf{t}^* = -\mathbf{Q}^\top (\mathbf{Q} \mathbf{Q}^\top)^{-1} \mathbf{I}_{\cdot, \mathcal{I}} \operatorname{sign}(\mathbf{s}'_{\mathcal{I}})$. Then, we obtain

$$\mathbf{y}_{\bar{\mathcal{I}}}^* = -\mathbf{I}_{\bar{\mathcal{I}}, \cdot} \left(\psi^{-2} \Phi^\top \Phi + \mathbf{I}_{\cdot, \bar{\mathcal{I}}} \mathbf{I}_{\bar{\mathcal{I}}, \cdot} \right)^{-1} \mathbf{I}_{\cdot, \mathcal{I}} \operatorname{sign}(\mathbf{s}'_{\mathcal{I}}),$$

which we can then bound as

$$\|\mathbf{y}_{\bar{\mathcal{I}}}^*\|_\infty \leq \left\| \left(\psi^{-2} \Phi^\top \Phi + \mathbf{I}_{\cdot, \bar{\mathcal{I}}} \mathbf{I}_{\bar{\mathcal{I}}, \cdot} \right)^{-1} \right\|_{\bar{\mathcal{I}}, \mathcal{I}} < 1,$$

where the final inequality is due to assumption (A1). Thus, there exists a vector $\mathbf{y} \in \operatorname{Im}(\Phi^\top)$ such that $\mathbf{y}_{\mathcal{I}} = \operatorname{sign}(\mathbf{s}'_{\mathcal{I}})$ and $\|\mathbf{y}_{\bar{\mathcal{I}}}\|_\infty < 1$, which satisfies the conditions for $\mathbf{s}' \in \tilde{\Omega}(\hat{\mathbf{s}})$.

By assumption (A2) of Theorem 1, $\hat{\Sigma}_{\cdot, \mathcal{I}}$ is full column rank, and thus so is $\Phi_{\cdot, \mathcal{I}}$. This guarantees that $\tilde{\Omega}(\hat{\mathbf{s}}) = \{\mathbf{s}'\}$, that is, \mathbf{s}' is the unique solution of (29). Since $\hat{\mathbf{s}} \in \tilde{\Omega}(\hat{\mathbf{s}})$, we have that $\mathbf{s}' = \hat{\mathbf{s}}$. Importantly, assumptions (A1) and (A2) do not rely on the choice of $\hat{\mathbf{s}} \in \hat{\Omega}$. Thus, \mathbf{s}' is the sole element of $\tilde{\Omega}(\hat{\mathbf{s}})$ for any $\hat{\mathbf{s}} \in \hat{\Omega}$, and therefore $\hat{\Omega} = \{\mathbf{s}'\}$.

Thus, we have shown that under (A1) and (A2) of Theorem 1, \mathbf{s}' is the unique solution of (28), and we can relax problem (27) for a convex problem (28) that has a unique solution equivalent to the desired solution \mathbf{s}' . Finally, recall that (27) and (28) are vectorized versions of (11) and (12), respectively, so this implies that $\hat{\mathbf{S}}_C = \mathbf{S}'_C$ for $\hat{\mathbf{S}}_C$ minimizing (12) and \mathbf{S}'_C minimizing (11), as desired. \blacksquare

Appendix C. Proof of Lemma 1

The following proof exploits the result in Claim 2 of (Navarro et al., 2022), which bounds the Frobenius norm of the commutator $\hat{\mathbf{C}}\mathbf{S}^* - \mathbf{S}^*\hat{\mathbf{C}}$ for a set of K graphs. In particular, we apply Claim 2 in (Navarro et al., 2022) for $K = 1$, which requires satisfying four conditions. However, as three are trivial for $K = 1$, we proceed with showing that the remaining condition is equivalent to 1) and 2) in the statement of Lemma 1.

For condition 4) of Theorem 2 of (Navarro et al., 2022), given that $K = 1$ we have that

$$\log N = o\left(\min\left\{\frac{M}{(\log M)^2}, M^{1/3}\right\}\right) = o(M^{1/3}),$$

since $M^{1/3} \leq M/(\log M)^2$ for every $M > 1$. \blacksquare

Appendix D. Proof of Lemma 2

For any $\mathbf{S} \in \mathcal{S}$, we let the matrix $\mathbf{S}^{(g)}$ denote the submatrix of \mathbf{S}^+ containing edges connecting nodes in group g for each $g \in [G]$ and $\mathbf{S}^{(g,h)}$ the submatrix containing edges connecting nodes between groups g and h for every $g, h \in [G]$ such that $g \neq h$. For any $\mathbf{S} \in \mathcal{S}$,

$$\begin{aligned} \|\mathbf{S}^+\|_1^2 &= \left(\sum_{g=1}^G \|\mathbf{S}^{(g)}\|_1 + \sum_{g \neq h} \|\mathbf{S}^{(g,h)}\|_1\right)^2 \leq \left(\sum_{g=1}^G \|\mathbf{S}^{(g)}\|_1\right)^2 + \left(\sum_{g \neq h} \|\mathbf{S}^{(g,h)}\|_1\right)^2 \\ &\leq 2 \left(\sum_{g=1}^G (N_g^2 - N_g)\right) \left(\sum_{g=1}^G \frac{\|\mathbf{S}^{(g)}\|_1^2}{(N_g^2 - N_g)^2}\right) + 2 \left(\sum_{g \neq h} N_g^2 N_h^2\right) \left(\sum_{g \neq h} \frac{\|\mathbf{S}^{(g,h)}\|_1^2}{N_g^2 N_h^2}\right) \\ &\leq 2 \left(\sum_{g \neq h} \frac{N_g^4}{G-1}\right) \left(\sum_{g \neq h} \frac{\|\mathbf{S}^{(g)}\|_1^2}{(N_g^2 - N_g)^2}\right) + 2 \left(\|\mathbf{Z}^\top \mathbf{1}\|_2^4 - \sum_{g=1}^G N_g^4\right) \left(\sum_{g \neq h} \frac{\|\mathbf{S}^{(g,h)}\|_1^2}{N_g^2 N_h^2}\right) \\ &\leq 2\|\mathbf{Z}^\top \mathbf{1}\|_2^4 \sum_{g \neq h} \left(\frac{\|\mathbf{S}^{(g)}\|_1}{N_g^2 - N_g}\right)^2 + \left(\frac{\|\mathbf{S}^{(g,h)}\|_1}{N_g N_h}\right)^2. \end{aligned}$$

Then, by the definition of $\|\mathbf{R}_G \mathbf{s}\|_2$ and the fact that $\|\mathbf{s}\|_1 = \frac{1}{2}\|\mathbf{S}^+\|_1$ for $\mathbf{s} = \text{vec}(\mathbf{S})_{\mathcal{L}}$,

$$\begin{aligned} \|\mathbf{s}\|_1^2 &\leq \frac{G^2 \|\mathbf{Z}^\top \mathbf{1}\|_2^4}{2} \|\mathbf{R}_G \mathbf{s}\|_2^2 + \|\mathbf{Z}^\top \mathbf{1}\|_2^4 \sum_{g \neq h} \frac{\|\mathbf{S}^{(g)}\|_1 \|\mathbf{S}^{(g,h)}\|_1}{(N_g^3 - N_g^2) N_h} \\ &\leq \frac{G^2 \|\mathbf{Z}^\top \mathbf{1}\|_2^4}{2} \|\mathbf{R}_G \mathbf{s}\|_2^2 + \frac{\|\mathbf{Z}^\top \mathbf{1}\|_2^4}{N_{\min}^2 - N_{\min}} \sum_{g=1}^G \|\mathbf{S}^{(g)}\|_F \sum_{h \neq g} \|\mathbf{S}^{(g,h)}\|_F \\ &\leq \frac{G^2 \|\mathbf{Z}^\top \mathbf{1}\|_2^4}{2} \|\mathbf{R}_G \mathbf{s}\|_2^2 + \frac{\|\mathbf{Z}^\top \mathbf{1}\|_2^4}{2(N_{\min}^2 - N_{\min})} \|\mathbf{S}^+\|_F^2 \\ &\leq \frac{G^2 \|\mathbf{Z}^\top \mathbf{1}\|_2^4}{2} \|\mathbf{R}_G \mathbf{s}\|_2^2 + \frac{\epsilon^2 \|\mathbf{Z}^\top \mathbf{1}\|_2^4}{\sigma_{\min}^2(\hat{\Sigma})(N_{\min}^2 - N_{\min})} \leq G^2 \|\mathbf{Z}^\top \mathbf{1}\|_2^4 \|\mathbf{R}_G \mathbf{s}\|_2^2 + \frac{2\epsilon^2 \|\mathbf{Z}^\top \mathbf{1}\|_2^4}{\sigma_{\min}^2(\hat{\Sigma}) N_{\min}^2}, \end{aligned}$$

allowing us to write (25) via the triangle inequality as desired. \blacksquare

Appendix E. Proof of Lemma 3

First, for any $\mathbf{S} \in \mathcal{S}$ with $\mathbf{s} = \text{vec}(\mathbf{S})_{\mathcal{L}}$ we have that

$$\|\mathbf{S}^+ \mathbf{1}\|_2^2 = \sum_{i=1}^N \left(\sum_{j=1}^N S_{ij}^+ \right)^2 \leq N \|\mathbf{S}^+\|_F^2 = 2N \|\mathbf{s}\|_2^2 \leq \frac{2N\epsilon^2}{\sigma_{\min}^2(\hat{\Sigma})} \quad (30)$$

since $\hat{\Sigma}$ is full column rank. Second, we have that

$$\|\mathbf{S}^+\|_1^2 = \left(\sum_{g=1}^G \|\mathbf{S}^+ \mathbf{z}^{(g)}\|_1 \right)^2 \leq \left(\sum_{g=1}^G \sqrt{N_g} \|\mathbf{S}^+ \mathbf{z}^{(g)}\|_2 \right)^2 \leq N_{\max} \|\mathbf{S}^+ \mathbf{Z}\|_F^2. \quad (31)$$

Then, by the definition of \mathbf{R}_N , we can lower bound $\|\mathbf{R}_N \mathbf{s}\|_2^2$ by terms containing $\|\mathbf{S}^+ \mathbf{1}\|_2^2$ and $\|\mathbf{S}^+ \mathbf{Z}\|_F^2$, that is,

$$\begin{aligned} \|\mathbf{R}_N \mathbf{s}\|_2^2 &= \frac{1}{GN} \sum_{g=1}^G \sum_{i=1}^N \left(\frac{[\mathbf{S}^+ \mathbf{z}^{(g)}]_i}{N_g} - \frac{1}{G-1} \sum_{h \neq g} \frac{[\mathbf{S}^+ \mathbf{z}^{(h)}]_i}{N_h} \right)^2 \\ &\geq \frac{1}{GN N_{\max}^2} \|\mathbf{S}^+ \mathbf{Z}\|_F^2 + \frac{1}{G(G-1)^2 N N_{\max}^2} \sum_{g=1}^G \|\mathbf{S}^+ (\mathbf{1} - \mathbf{z}^{(g)})\|_2^2 \\ &\quad - \frac{2}{G(G-1) N N_{\min}^2} \sum_{g=1}^G (\mathbf{S}^+ \mathbf{z}^{(g)})^\top \mathbf{S}^+ (\mathbf{1} - \mathbf{z}^{(g)}) \\ &= \frac{1}{GN N_{\max}^2} \|\mathbf{S}^+ \mathbf{Z}\|_F^2 + \frac{(G-2) \|\mathbf{S}^+ \mathbf{1}\|_2^2}{G(G-1)^2 N N_{\max}^2} + \frac{1}{G(G-1)^2 N N_{\max}^2} \|\mathbf{S}^+ \mathbf{Z}\|_F^2 \\ &\quad - \frac{2}{G(G-1) N N_{\min}^2} (\|\mathbf{S}^+ \mathbf{1}\|_2^2 - \|\mathbf{S}^+ \mathbf{Z}\|_F^2) \\ &\geq \frac{G}{(G-1)^2 N N_{\max}^2} \|\mathbf{S}^+ \mathbf{Z}\|_F^2 \frac{2}{G(G-1) N N_{\min}^2} \|\mathbf{S}^+ \mathbf{1}\|_2^2. \end{aligned} \quad (32)$$

With (30), (31), and (32), we bound $\|\mathbf{R}_N \mathbf{s}\|_2^2$ below by $\|\mathbf{S}^+\|_1^2$ with

$$\|\mathbf{R}_N \mathbf{s}\|_2^2 \geq \frac{1}{(G-1)^2 N N_{\max}^3} \|\mathbf{S}^+\|_1^2 - \frac{4\epsilon^2}{G(G-1) N_{\min}^2 \sigma_{\min}^2(\hat{\Sigma})},$$

which implies that

$$\begin{aligned} \|\mathbf{S}^+\|_1^2 &\leq (G-1)^2 N N_{\max}^3 \|\mathbf{R}_N \mathbf{s}\|_2^2 + \frac{4(G-1) N N_{\max}^3 \epsilon^2}{G N_{\min}^2 \sigma_{\min}^2(\hat{\Sigma})} \\ &\leq G^2 N N_{\max}^3 \|\mathbf{R}_N \mathbf{s}\|_2^2 + \frac{4 N N_{\max}^3 \epsilon^2}{N_{\min}^2 \sigma_{\min}^2(\hat{\Sigma})} \leq G^3 N_{\max}^4 \|\mathbf{R}_N \mathbf{s}\|_2^2 + \frac{4 G N_{\max}^4 \epsilon^2}{N_{\min}^2 \sigma_{\min}^2(\hat{\Sigma})} \end{aligned}$$

yielding the inequality in (26) by the triangle inequality and since $\|\mathbf{S}^+\|_1^2 = 4\|\mathbf{s}\|_1^2$. ■

Appendix F. Proof of Theorem 2

We bound the error between the estimate $\hat{\mathbf{S}}_C$ and \mathbf{S}^* via the vectorizations $\hat{\mathbf{s}}$ as the solution to (28) for $\mathbf{R} = \mathbf{R}_G$ and $\mathbf{s}^* = \text{vec}(\mathbf{S}^*)_{\mathcal{L}}$. Note that since $\hat{\Sigma}$ is full column rank, then the problem (28) has a unique solution, that is, its solution set is a singleton $\hat{\Omega} = \{\hat{\mathbf{s}}\}$ (Shafipour and Mateos, 2020, Proposition 2).

To relate the error $\|\hat{\mathbf{s}} - \mathbf{s}^*\|_1$ to the sparsity in \mathbf{s}^* , we define $\mathcal{K} := \text{supp}(\mathbf{s}^*)$ along with the vector $\hat{\mathbf{u}} \in \mathbb{R}^{N(N-1)/2}$ to minimize the distance

$$\hat{\mathbf{u}} := \underset{\mathbf{u}}{\text{argmin}} \|\hat{\mathbf{s}} - \mathbf{u}\|_1 \text{ s.t. } \text{supp}(\mathbf{u}) \subseteq \mathcal{K},$$

and we proceed with bounding the distance $\xi := \|\hat{\mathbf{s}} - \hat{\mathbf{u}}\|_1$. We have that

$$\begin{aligned} \xi &= \min_{\mathbf{u}} \|\hat{\mathbf{s}} - \mathbf{u}\|_1 \text{ s.t. } \text{supp}(\mathbf{u}) \subseteq \mathcal{K} \\ &= \max_{\mathbf{v}} \min_{\mathbf{u}} \|\hat{\mathbf{s}} - \mathbf{u}\|_1 + \mathbf{v}^\top \mathbf{u}_{\bar{\mathcal{K}}} \\ &= \max_{\mathbf{w}} \min_{\mathbf{u}} \|\hat{\mathbf{s}} - \mathbf{u}\|_1 + \mathbf{w}^\top \mathbf{u} \text{ s.t. } \text{supp}(\mathbf{w}) \subseteq \bar{\mathcal{K}}, \|\mathbf{w}\|_\infty \leq 1, \end{aligned}$$

where we require that $\|\mathbf{w}\|_\infty \leq 1$, otherwise an entry of $\hat{\mathbf{u}}$ may be $-\infty$, yielding unbounded minimization of ξ . Then, we have that

$$\begin{aligned} \xi &\leq \max_{\mathbf{w}} \mathbf{w}^\top \hat{\mathbf{s}} \text{ s.t. } \text{supp}(\mathbf{w}) \subseteq \bar{\mathcal{K}}, \|\mathbf{w}\|_\infty \leq 1 \\ &= \max_{\mathbf{w}} (\text{sign}(\mathbf{s}^*) + \mathbf{w})^\top \hat{\mathbf{s}} - \text{sign}(\mathbf{s}^*)^\top \hat{\mathbf{s}} \text{ s.t. } \text{supp}(\mathbf{w}) \subseteq \bar{\mathcal{K}}, \|\mathbf{w}\|_\infty \leq 1 \\ &\leq \|\hat{\mathbf{s}}\|_1 - \|\mathbf{s}^*\|_1 + \text{sign}(\mathbf{s}^*)^\top (\mathbf{s}^* - \hat{\mathbf{s}}), \end{aligned}$$

where the last inequality arises because $\text{sign}(\mathbf{s}^*)$ and \mathbf{w} have non-overlapping supports and $\|\mathbf{w}\|_\infty \leq 1$, so $(\text{sign}(\mathbf{s}^*) + \mathbf{w})^\top \hat{\mathbf{s}} \leq \|\hat{\mathbf{s}}\|_1$, and $\text{sign}(\mathbf{s}^*)^\top \mathbf{s}^* = \|\mathbf{s}^*\|_1$. Moreover, as $\hat{\Sigma}$ is full column rank,

$$\begin{aligned} \xi &\leq \|\hat{\mathbf{s}}\|_1 - \|\mathbf{s}^*\|_1 + \|(\mathbf{s}^* - \hat{\mathbf{s}})_{\mathcal{K}}\|_1 \leq \|\hat{\mathbf{s}}\|_1 - \|\mathbf{s}^*\|_1 + \sqrt{|\mathcal{K}|} \|\mathbf{s}^* - \hat{\mathbf{s}}\|_2 \\ &\leq \|\hat{\mathbf{s}}\|_1 - \|\mathbf{s}^*\|_1 + \frac{\sqrt{|\mathcal{K}|}}{\sigma_{\min}(\hat{\Sigma})} \|\hat{\Sigma}(\mathbf{s}^* - \hat{\mathbf{s}})\|_2 \leq \|\hat{\mathbf{s}}\|_1 - \|\mathbf{s}^*\|_1 + \frac{2\epsilon\sqrt{|\mathcal{K}|}}{\sigma_{\min}(\hat{\Sigma})}, \end{aligned} \quad (33)$$

where the final equality is by Lemma 1. With our bound for $\xi = \|\hat{\mathbf{s}} - \hat{\mathbf{u}}\|_1$, we can also bound the distance $\|\mathbf{s}^* - \hat{\mathbf{u}}\|_1$. Since $\text{supp}(\hat{\mathbf{u}}) \subseteq \mathcal{K}$ and $k \geq \sqrt{|\mathcal{K}|}$ by Assumption (A4),

$$\begin{aligned} \|\mathbf{s}^* - \hat{\mathbf{u}}\|_1 &\leq k\|\mathbf{s}^* - \hat{\mathbf{u}}\|_2 \leq k\|\hat{\mathbf{s}} - \hat{\mathbf{u}}\|_1 + k\|\mathbf{s}^* - \hat{\mathbf{s}}\|_2 \\ &\leq k\|\hat{\mathbf{s}} - \hat{\mathbf{u}}\|_1 + \frac{k}{\sigma_{\min}(\hat{\Sigma})} \|\hat{\Sigma}(\mathbf{s}^* - \hat{\mathbf{s}})\|_2 \leq k\|\hat{\mathbf{s}} - \hat{\mathbf{u}}\|_1 + \frac{2k\epsilon}{\sigma_{\min}(\hat{\Sigma})}. \end{aligned}$$

Then, by the definition of ξ and (33) we have that

$$\begin{aligned} \|\hat{\mathbf{s}} - \mathbf{s}^*\|_1 &\leq \xi + \|\mathbf{s}^* - \hat{\mathbf{u}}\|_1 \\ &\leq (1+k)\xi + \frac{2k\epsilon}{\sigma_{\min}(\hat{\Sigma})} \leq (1+k)(\|\hat{\mathbf{s}}\|_1 - \|\mathbf{s}^*\|_1) + (2+k)\frac{2k\epsilon}{\sigma_{\min}(\hat{\Sigma})}. \end{aligned} \quad (34)$$

Note that if \mathbf{s}^* is a feasible solution of (28), then $\|\hat{\mathbf{s}}\|_1 \leq \|\mathbf{s}^*\|_1$ by the optimality of $\hat{\mathbf{s}}$, and the error bound consists only of the second term in the right-hand side of (34). This proves the lower and upper bounds in (14) and (15), respectively, when $R_G(\mathbf{S}^*) \leq \tau^2$. Thus, we proceed with bounding the error when \mathbf{s}^* is not feasible, that is, $R_G(\mathbf{S}^*) > \tau^2$.

By Lemma 2, if $\|\mathbf{R}_G \mathbf{s}^*\|_2 > \tau$ then

$$\|\hat{\mathbf{S}} - \mathbf{S}^*\|_1 = 2\|\hat{\mathbf{s}} - \mathbf{s}^*\|_1 \leq \frac{4k\epsilon(2+k)}{\sigma_{\min}(\hat{\Sigma})} + 2G\|\mathbf{Z}^\top \mathbf{1}\|_2^2(1+k)\|\mathbf{R}\mathbf{s}^*\|_2 + \frac{4\epsilon\|\mathbf{Z}^\top \mathbf{1}\|_2^2(1+k)}{\sigma_{\min}(\hat{\Sigma})N_{\min}},$$

equivalent to the upper bound in (15) when $R_G(\mathbf{S}^*) = \|\mathbf{R}_G \mathbf{s}^*\|_2^2 > \tau^2$.

We then move on to demonstrating the lower bound in (14). For any $\mathbf{S} \in \mathcal{S}$, $\mathbf{S}^{(g)} \in \mathbb{R}^{N_g \times N_g}$ denotes the submatrix of \mathbf{S}^+ containing edges connecting nodes in group g for every $g \in [G]$. Similarly, for every $g, h \in [G]$ such that $g \neq h$, $\mathbf{S}^{(g,h)} \in \mathbb{R}^{N_g \times N_h}$ is the submatrix of \mathbf{S} containing edges connecting nodes between groups g and h . By the definition of \mathbf{R}_G and the fact that $\mathbf{S} \geq \mathbf{0}$,

$$\begin{aligned} \|\mathbf{R}_G \mathbf{s}\|_2^2 &= \frac{1}{G^2 - G} \sum_{g \neq h} \left(\frac{\mathbf{1}^\top \mathbf{S}^{(g)} \mathbf{1}}{N_g^2 - N_g} - \frac{\mathbf{1}^\top \mathbf{S}^{(g,h)} \mathbf{1}}{N_g N_h} \right)^2 \\ &\leq \frac{1}{G^2 - G} \sum_{g \neq h} \left(\frac{\|\mathbf{S}^{(g)}\|_1}{N_g^2 - N_g} \right)^2 + \left(\frac{\|\mathbf{S}^{(g,h)}\|_1}{N_g N_h} \right)^2 \\ &\leq \frac{1}{G^2 - G} \sum_{g \neq h} \left(\frac{\|\mathbf{S}^{(g)}\|_F^2}{N_g^2 - N_g} + \frac{\|\mathbf{S}^{(g,h)}\|_F^2}{N_g N_h} \right) \\ &\leq \frac{1}{G(N_{\min} - 1)^2} \left(\sum_{g=1}^G \|\mathbf{S}^{(g)}\|_F^2 + \sum_{g \neq h} \|\mathbf{S}^{(g,h)}\|_F^2 \right) \\ &= \frac{1}{G(N_{\min} - 1)^2} \|\mathbf{S}^+\|_F^2 \leq \frac{4}{GN_{\min}^2} \|\mathbf{S}\|_F^2. \end{aligned}$$

Then, we have that

$$\|\hat{\mathbf{S}} - \mathbf{S}^*\|_1 \geq \|\hat{\mathbf{S}} - \mathbf{S}^*\|_F \geq \frac{N_{\min} \sqrt{G}}{2} \|\mathbf{R}_G(\hat{\mathbf{s}} - \mathbf{s}^*)\|_2 \geq \frac{N_{\min} \sqrt{G}}{2} (\|\mathbf{R}_G \mathbf{s}^*\|_2 - \tau),$$

yielding the result in (14) as desired since $\sqrt{R_G(\mathbf{S}^*)} = \|\mathbf{R}_G \mathbf{s}^*\|_2$ and $\|\hat{\mathbf{S}} - \mathbf{S}^*\|_1 \geq 0$. ■

Appendix G. Proof of Theorem 3

As in Appendix F, we bound the error between $\hat{\mathbf{S}}_C$ and \mathbf{S}^* via the vectorizations $\hat{\mathbf{s}}$ and \mathbf{s}^* for $\mathbf{R} = \mathbf{R}_N$. We may repeat the steps in the proof of Theorem 2 until equation (34). As before, when $R_N(\mathbf{S}^*) \leq \tau^2$, the target \mathbf{s}^* is a feasible solution of (28), and we obtain the upper and lower error bounds in (17) and (16), respectively, when $R_N(\mathbf{S}^*) \leq \tau^2$. We then continue with the case when $R_N(\mathbf{S}^*) > \tau^2$. By Lemma 3, if $\|\mathbf{R}_N \mathbf{s}^*\|_2 > \tau$ then

$$\begin{aligned} \|\hat{\mathbf{S}} - \mathbf{S}^*\|_1 &= 2\|\hat{\mathbf{s}} - \mathbf{s}^*\|_1 \\ &\leq \frac{4k\epsilon(2+k)}{\sigma_{\min}(\hat{\Sigma})} + \frac{2\epsilon N_{\max}^2 \sqrt{G}(1+k)}{\sigma_{\min}(\hat{\Sigma})N_{\min}} + GN_{\max}^2 \sqrt{G}(1+k)\|\mathbf{R}_N \mathbf{s}^*\|_2, \end{aligned}$$

yielding the upper bound in (17) when $R_N(\mathbf{S}^*) = \|\mathbf{R}_N \mathbf{S}^*\|_2^2 > \tau^2$.

For the lower bound in (16), we use the definition of \mathbf{R}_N and $\mathbf{S} \geq \mathbf{0}$ to get

$$\begin{aligned}
 \|\mathbf{R}_N \mathbf{s}\|_2^2 &= \frac{1}{GN} \sum_{g=1}^G \sum_{i=1}^N \left(\frac{[\mathbf{S}^+ \mathbf{z}^{(g)}]_i}{N_g} - \frac{1}{G-1} \sum_{h \neq g} \frac{[\mathbf{S}^+ \mathbf{z}^{(h)}]_i}{N_h} \right)^2 \\
 &\leq \frac{1}{GN} \sum_{g=1}^G \sum_{i=1}^N \frac{[\mathbf{S}^+ \mathbf{z}^{(g)}]_i^2}{N_g^2} + \frac{1}{G(G-1)^2 N} \sum_{g=1}^G \sum_{i=1}^N \left(\sum_{h \neq g} \frac{[\mathbf{S}^+ \mathbf{z}^{(h)}]_i}{N_h} \right)^2 \\
 &\leq \frac{1}{GN N_{\min}^2} \|\mathbf{S}^+ \mathbf{Z}\|_F^2 + \frac{1}{G(G-1)^2 N N_{\min}^2} \sum_{g=1}^G \|\mathbf{S}^+ (\mathbf{1} - \mathbf{z}^{(g)})\|_2^2 \\
 &\leq \frac{1}{GN N_{\min}^2} \|\mathbf{S}^+ \mathbf{Z}\|_F^2 + \frac{G-2}{G(G-1)^2 N N_{\min}^2} \|\mathbf{S}^+ \mathbf{1}\|_2^2 + \frac{1}{G(G-1)^2 N N_{\min}^2} \|\mathbf{S}^+ \mathbf{Z}\|_F^2 \\
 &\leq \left(\frac{1}{GN N_{\min}^2} + \frac{1}{G(G-1) N N_{\min}^2} \right) \|\mathbf{S}^+\|_1^2 \\
 &\leq \frac{2}{(G-1) N N_{\min}^2} \|\mathbf{S}^+\|_1^2 \leq \frac{4}{GN N_{\min}^2} \|\mathbf{S}\|_1^2,
 \end{aligned}$$

which gives

$$\|\hat{\mathbf{S}} - \mathbf{S}^*\|_1 \geq \frac{N_{\min} \sqrt{GN}}{2} \|\mathbf{R}_N(\hat{\mathbf{s}} - \mathbf{s}^*)\|_2 \geq \frac{N_{\min} \sqrt{GN}}{2} (\|\mathbf{R}_N \mathbf{s}^*\|_2 - \tau),$$

as in (16) as desired for $R_N(\mathbf{S}^*) > \tau^2$. ■

Appendix H. Proof of Theorem 4

The proof follows analogous steps to the proof of Theorem 1 in Appendix B. We again proceed only for $\mathcal{S} = \mathcal{S}_A$, but the result also holds for $\mathcal{S} = \mathcal{S}_L$, as discussed in Appendix I.

First, consider the following vectorization of (19)

$$\mathbf{s}', \boldsymbol{\lambda}'_V \in \underset{\mathbf{s}, \boldsymbol{\lambda}}{\operatorname{argmin}} \quad \|\mathbf{s}\|_0 \quad \text{s.t.} \quad \|\mathbf{U}\mathbf{s} - \hat{\mathbf{J}}\boldsymbol{\lambda}\|_2 \leq \epsilon, \quad \|\mathbf{R}\mathbf{s}\|_2 \leq \tau, \quad \mathbf{E}\mathbf{s} \geq \mathbf{1}, \quad \mathbf{s} \geq \mathbf{0}, \quad (35)$$

whose optimal set of GSOs can also be obtained via

$$\mathbf{s}' \in \underset{\mathbf{s}}{\operatorname{argmin}} \quad \|\mathbf{s}\|_0 \quad \text{s.t.} \quad \|\mathbf{U}\mathbf{s} - \hat{\mathbf{J}}\hat{\mathbf{J}}^\top \mathbf{U}\mathbf{s}\|_2 \leq \epsilon, \quad \|\mathbf{R}\mathbf{s}\|_2 \leq \tau, \quad \mathbf{E}\mathbf{s} \geq \mathbf{1}, \quad \mathbf{s} \geq \mathbf{0} \quad (36)$$

since the pseudo-inverse of $\hat{\mathbf{J}}$ is $\hat{\mathbf{J}}^\dagger = \hat{\mathbf{J}}^\top$ (Segarra et al., 2017). Indeed, for any solution $(\mathbf{s}'_1, \boldsymbol{\lambda}'_1)$ of (35), \mathbf{s}'_1 is feasible for (36), and therefore $\|\mathbf{s}'_1\|_0 \leq \|\mathbf{s}'_2\|_0$ for any solution \mathbf{s}'_2 of (36). Conversely, $(\mathbf{s}'_2, \hat{\mathbf{J}}^\top \mathbf{U}\mathbf{s}'_2)$ is a feasible solution of (35), therefore $\|\mathbf{s}'_1\|_0 \leq \|\mathbf{s}'_2\|_0$, so (35) and (36) share the same optimal vectorized GSOs. We also vectorize (20) as

$$\hat{\Omega} = \underset{\mathbf{s}}{\operatorname{argmin}} \quad \|\mathbf{s}\|_1 \quad \text{s.t.} \quad \|\hat{\mathbf{F}}\mathbf{s}\|_2 \leq \epsilon, \quad \|\mathbf{R}\mathbf{s}\|_2 \leq \tau, \quad \mathbf{E}\mathbf{s} \geq \mathbf{1}, \quad \mathbf{s} \geq \mathbf{0}. \quad (37)$$

The remainder of the proof follows the same steps as in Appendix B. ■

Appendix I. Fair Spectral Templates with Graph Laplacian

Here, we introduce analogous theoretical results for graph Laplacian GSOs $\mathcal{S} = \mathcal{S}_L$.

I.1 FairSpecTemp Convex Relaxation

We introduce $\hat{\Sigma}_L := [\hat{\mathbf{C}} \oplus (-\hat{\mathbf{C}})]_{\cdot, \mathcal{D}} \mathbf{E} + \hat{\Sigma}$ such that $\|\hat{\mathbf{C}}\mathbf{S} - \mathbf{S}\hat{\mathbf{C}}\|_F = \|\hat{\Sigma}_L \mathbf{s}\|_2$ for $\mathbf{S} \in \mathcal{S}_L$ and $\mathbf{s} = \text{vec}(\mathbf{S})_{\mathcal{L}}$. Then, we adapt the result on the convex relaxation of (11) in Theorem 1 for $\mathcal{S} = \mathcal{S}_L$ as follows.

Corollary 1 *If problems (11) and (12) are feasible for $\mathcal{S} = \mathcal{S}_L$, then for \mathbf{S}'_C as a solution to (11), we have that $\hat{\mathbf{S}}_C = \mathbf{S}'_C$ is the unique solution to (12) if*

(A1) *The submatrix $[\hat{\Sigma}_L]_{\cdot, \mathcal{I}}$ is full column rank, and*

(A2) *There exists a constant $\psi > 0$ such that*

$$\left\| \left(\psi^{-2} \Phi^\top \Phi + \mathbf{I}_{\cdot, \bar{\mathcal{I}}} \mathbf{I}_{\bar{\mathcal{I}}, \cdot} \right)^{-1} \right\|_{\bar{\mathcal{I}}, \mathcal{I}} < 1, \quad (38)$$

where $\mathcal{I} = \text{supp}(\mathbf{s}')$ for $\mathbf{s}' = \text{vec}(\mathbf{S}'_C)_{\mathcal{L}}$, and $\Phi := [\hat{\Sigma}_L^\top, \mathbf{R}^\top, \mathbf{E}^\top]^\top$.

Proof Observe that the equivalent vectorization of (11) for $\mathcal{S} = \mathcal{S}_L$ is

$$\mathbf{s}' \in \underset{\mathbf{s}}{\operatorname{argmin}} \quad \|\mathbf{s}\|_0 \quad \text{s.t.} \quad \|\hat{\Sigma}_L \mathbf{s}\|_2 \leq \epsilon, \quad \|\mathbf{R}\mathbf{s}\|_2 \leq \tau, \quad -\mathbf{E}\mathbf{s} \geq \mathbf{1}, \quad \mathbf{s} \leq \mathbf{0},$$

so an analogous procedure with the same auxiliary problem (29) yields the same guarantee. \blacksquare

Similarly, we adapt Theorem 4 on the convex relaxation of (19) for $\mathcal{S} = \mathcal{S}_L$. To this end, we define $\hat{\mathbf{F}}_L := [\mathbf{I} - \hat{\mathbf{J}}\hat{\mathbf{J}}^\top]_{\cdot, \mathcal{D}} \mathbf{E} + \hat{\mathbf{F}}$.

Corollary 2 *If problems (19) and (20) are feasible for $\mathcal{S} = \mathcal{S}_L$, then for \mathbf{S}'_V as a solution to (19), we have that $\hat{\mathbf{S}}_V = \mathbf{S}'_V$ is the unique solution to (20) if*

(A1) *The submatrix $[\hat{\mathbf{F}}_L]_{\cdot, \mathcal{I}}$ is full column rank, and*

(A2) *There exists a constant $\psi > 0$ such that*

$$\left\| \left(\psi^{-2} \Psi^\top \Psi + \mathbf{I}_{\cdot, \bar{\mathcal{I}}} \mathbf{I}_{\bar{\mathcal{I}}, \cdot} \right)^{-1} \right\|_{\bar{\mathcal{I}}, \mathcal{I}} < 1, \quad (39)$$

where $\mathcal{I} = \text{supp}(\mathbf{s}')$ for $\mathbf{s}' = \text{vec}(\mathbf{S}'_V)_{\mathcal{L}}$, and $\Psi := [\hat{\mathbf{F}}_L^\top, \mathbf{R}, \mathbf{E}^\top]^\top$.

The proof of Corollary 2 is analogous to that of Corollary 1 and is thus omitted.

I.2 FairSpecTemp Error Bound

Let conditions $(A1)$, $(A2)$, and $(A4)$ hold from Assumption 1, and let $\hat{\Sigma}_L$ be full column rank, analogous to condition $(A3)$. To see why the error bounds in Theorems 2 and 3 are equivalent for $\mathcal{S} = \mathcal{S}_A$ and $\mathcal{S} = \mathcal{S}_L$ up to a scaling, first observe that by the proofs of the lower bounds in (14) and (16), we obtain the same results if $\text{diag}(\mathbf{S}) \neq \mathbf{0}$. Then, for the upper bounds in (15) and (17) and $\hat{\mathbf{S}}, \mathbf{S}^* \in \mathcal{S}_L$, observe that

$$\begin{aligned}\|\hat{\mathbf{S}} - \mathbf{S}^*\|_1 &\leq \|(\hat{\mathbf{S}} - \mathbf{S}^*)^+\|_1 + \|(\hat{\mathbf{S}} - \mathbf{S}^*)^-\|_1 \\ &= 2\|\hat{\mathbf{s}} - \mathbf{s}^*\|_1 + \|\mathbf{E}(\hat{\mathbf{s}} - \mathbf{s}^*)\|_1 \\ &\leq (2 + \sigma_{\max}(\mathbf{E}))\|\hat{\mathbf{s}} - \mathbf{s}^*\|_1,\end{aligned}$$

thus the upper bounds from Theorems 2 and 3 are scaled by $\frac{2 + \sigma_{\max}(\mathbf{E})}{2}$ for $\mathcal{S} = \mathcal{S}_L$ with the assumption that $\hat{\Sigma}_L$ is full column rank, which allows us to repeat the steps in Appendices F and G for the proofs of Theorems 2 and 3, respectively.

References

Massimo A. Achterberg, Bastian Prasse, Long Ma, Stojan Trajanovski, Maksim Kitsak, and Piet Van Mieghem. Comparing the accuracy of several network-based COVID-19 prediction algorithms. *International Journal of Forecasting*, 38(2):489–504, 2022.

Chirag Agarwal, Himabindu Lakkaraju, and Marinka Zitnik. Towards a unified framework for fair and stable graph representation learning. In *Conference on Uncertainty in Artificial Intelligence (UAI)*, volume 161, pages 2114–2124. PMLR, 2021.

Adrian Arnaiz-Rodriguez, Georgina Curto Rex, and Nuria Oliver. Structural group unfairness: Measurement and mitigation by means of the effective resistance. In *International AAAI Conference on Web and Social Media (ICWSM)*, volume 19, pages 83–106, 2025.

Brian Baingana and Georgios B. Giannakis. Tracking switched dynamic network topologies from information cascades. *IEEE Transactions on Signal Processing*, 65(4):985–997, 2017.

Amir Beck and Marc Teboulle. A fast iterative shrinkage-thresholding algorithm for linear inverse problems. *SIAM Journal on Imaging Sciences*, 2(1):183–202, 2009.

Kamal Berahmand, Farid Saberi-Movahed, Razieh Sheikhpour, Yuefeng Li, and Mahdi Jalili. A comprehensive survey on spectral clustering with graph structure learning. *arXiv preprint arXiv:2501.13597*, 2025.

Alex Beutel, Jilin Chen, Tulsee Doshi, Hai Qian, Li Wei, Yi Wu, Lukasz Heldt, Zhe Zhao, Lichan Hong, Ed H. Chi, and Cristos Goodrow. Fairness in recommendation ranking through pairwise comparisons. In *International Conference on Knowledge Discovery and Data Mining (SIGKDD)*, pages 2212–2220. ACM, 2019.

Avishhek Bose and William Hamilton. Compositional fairness constraints for graph embeddings. In *International Conference on Machine Learning (ICML)*, volume 97, pages 715–724. PMLR, 2019.

Styliani Bourli and Evangelia Pitoura. Bias in knowledge graph embeddings. In *IEEE/ACM International Conference Advances in Social Networks Analysis and Mining (ASONAM)*, pages 6–10. IEEE, 2020.

Sylvain Bouveret, Katarína Cechlárová, Edith Elkind, Ayumi Igarashi, and Dominik Peters. Fair division of a graph. In *International Joint Conference on Artificial Intelligence*, pages 135–141, 2017.

Ivan Brugere, Brian Gallagher, and Tanya Y. Berger-Wolf. Network structure inference, a survey: Motivations, methods, and applications. *ACM Computing Surveys (CSUR)*, 51(2):1–39, 2019.

A. Buciulea, S. Rey, and A. G. Marques. Learning graphs from smooth and graph-stationary signals with hidden variables. *IEEE Transactions on Signal Information Processing over Networks*, 8:273–287, 2022.

Andrei Buciulea, Jiaxi Ying, Antonio G. Marques, and Daniel P. Palomar. Polynomial graphical lasso: Learning edges from Gaussian graph-stationary signals. *IEEE Transactions on Signal Processing*, 73:1153–1167, 2025.

Maarten Buyl and Tijl De Bie. DeBayes: A Bayesian method for debiasing network embeddings. In *International Conference on Machine Learning (ICML)*, volume 119, pages 1220–1229. PMLR, 2020.

Maarten Buyl and Tijl De Bie. The KL-divergence between a graph model and its fair I-projection as a fairness regularizer. In *Joint European Conference on Machine Learning and Knowledge Discovery in Databases (ECML PKDD)*, volume 12976, pages 351–366. Springer, 2021.

Xiaodong Cai, Juan Andrés Bazerque, and Georgios B. Giannakis. Inference of gene regulatory networks with sparse structural equation models exploiting genetic perturbations. *PLoS Computational Biology*, 9(5):e1003068, 2013.

José Vinícius de Miranda Cardoso and Daniel P. Palomar. Learning undirected graphs in financial markets. In *Asilomar Conference Signals, Systems, and Computers*, pages 741–745, 2020.

Serina Chang, Emma Pierson, Pang Wei Koh, Joline Gerardin, Beth Redbird, David Grusky, and Jure Leskovec. Mobility network models of COVID-19 explain inequities and inform reopening. *Nature*, 589(7840):82–87, 2021.

April Chen, Ryan Rossi, Nedim Lipka, Jane Hoffswell, Gromit Chan, Shunan Guo, Eunyee Koh, Sungchul Kim, and Nesreen K. Ahmed. Graph learning with localized neighborhood fairness. *arXiv preprint arXiv:2212.12040*, 2022.

Alexandra Chouldechova. Fair prediction with disparate impact: A study of bias in recidivism prediction instruments. *Big Data*, 5(2):153–163, 2017.

George Christodoulou, Amos Fiat, Elias Koutsoupias, and Alkmini Sgouritsa. Fair allocation in graphs. In *The ACM Conference on Economics and Computation (EC)*, pages 473–488. ACM, 2023.

Sean Current, Yuntian He, Saket Gurukar, and Srinivasan Parthasarathy. FairEGM: Fair link prediction and recommendation via emulated graph modification. In *Equity and Access in Algorithms, Mechanisms, and Optimization*, pages 1–14. ACM, 2022.

Lital Dabush and Tirza Routtenberg. Verifying the smoothness of graph signals: A graph signal processing approach. *IEEE Transactions on Signal Processing*, 72:4349–4365, 2024.

Enyan Dai and Suhang Wang. Say no to the discrimination: Learning fair graph neural networks with limited sensitive attribute information. In *ACM International Conference on Web Search and Data Mining*, pages 680–688. ACM, 2021.

Petar Djuric and Cédric Richard. *Cooperative and Graph Signal Processing: Principles and Applications*. Academic Press, 2018.

Xiaowen Dong, Dorina Thanou, Pascal Frossard, and Pierre Vandergheynst. Learning Laplacian matrix in smooth graph signal representations. *IEEE Transactions on Signal Processing*, 64(23):6160–6173, 2016.

Xiaowen Dong, Dorina Thanou, Michael Rabbat, and Pascal Frossard. Learning graphs from data: A signal representation perspective. *IEEE Signal Processing Magazine*, 36(3):44–63, 2019.

Yushun Dong, Jian Kang, Hanghang Tong, and Jundong Li. Individual fairness for graph neural networks: A ranking based approach. In *International Conference on Knowledge Discovery and Data Mining (SIGKDD)*, pages 300–310. ACM, 2021.

Yushun Dong, Ninghao Liu, Brian Jalaian, and Jundong Li. EDITS: Modeling and mitigating data bias for graph neural networks. In *ACM Web Conference*, pages 1259–1269. ACM, 2022a.

Yushun Dong, Song Wang, Yu Wang, Tyler Derr, and Jundong Li. On structural explanation of bias in graph neural networks. In *International Conference on Knowledge Discovery and Data Mining (SIGKDD)*, pages 316–326. ACM, 2022b.

Yushun Dong, Jing Ma, Song Wang, Chen Chen, and Jundong Li. Fairness in graph mining: A survey. *IEEE Transactions on Knowledge and Data Engineering*, 35(10):10583–10602, 2023a.

Yushun Dong, Song Wang, Jing Ma, Ninghao Liu, and Jundong Li. Interpreting unfairness in graph neural networks via training node attribution. In *AAAI Conference on Artificial Intelligence*, volume 37, pages 7441–7449, 2023b.

Tomislav Duricic, Dominik Kowald, Emanuel Lacic, and Elisabeth Lex. Beyond-accuracy: A review on diversity, serendipity, and fairness in recommender systems based on graph neural networks. *Frontiers in Big Data*, 6:1251072, 2023.

Cynthia Dwork, Moritz Hardt, Toniann Pitassi, Omer Reingold, and Richard Zemel. Fairness through awareness. In *Innovations in Theoretical Computer Science Conference*, page 214–226, 2012.

Damien R. Farine and Hal Whitehead. Constructing, conducting and interpreting animal social network analysis. *Journal of Animal Ecology*, 84(5):1144–1163, 2015.

Michael Feldman, Sorelle A Friedler, John Moeller, Carlos Scheidegger, and Suresh Venkatasubramanian. Certifying and removing disparate impact. In *International Conference on Knowledge Discovery and Data Mining (SIGKDD)*, page 259–268. ACM, 2015.

Beatrice Franzolini, Alexandros Beskos, Maria De Iorio, Warrick Poklewski Koziell, and Karolina Grzeszkiewicz. Change point detection in dynamic Gaussian graphical models: The impact of COVID-19 pandemic on the U.S. stock market. *The Annals of Statistics*, 18(1), 2024.

Jerome Friedman, Trevor Hastie, and Robert Tibshirani. Sparse inverse covariance estimation with the graphical lasso. *Biostatistics*, 9(3):432–441, 2008.

Zuohui Fu, Yikun Xian, Ruoyuan Gao, Jieyu Zhao, Qiaoying Huang, Yingqiang Ge, Shuyuan Xu, Shijie Geng, Chirag Shah, Yongfeng Zhang, and Gerard De Melo. Fairness-aware explainable recommendation over knowledge graphs. In *International ACM SIGIR Conference on Research and Development in Information Retrieval*, pages 69–78. ACM, 2020.

Fernando Gama, Antonio G. Marques, Geert Leus, and Alejandro Ribeiro. Convolutional neural network architectures for signals supported on graphs. *IEEE Transactions on Signal Processing*, 67(4):1034–1049, 2019.

Benjamin Girault, Paulo Gonçalves, and Éric Fleury. Translation on graphs: An isometric shift operator. *IEEE Signal Processing Letters*, 22(12):2416–2420, 2015.

Shubham Gupta and Ambedkar Dukkipati. Consistency of constrained spectral clustering under graph induced fair planted partitions. In *Advances in Neural Information Processing Systems*, volume 35, pages 13527–13540. Curran Associates, Inc., 2022.

Yosh Halberstam and Brian Knight. Homophily, group size, and the diffusion of political information in social networks: Evidence from Twitter. *Journal of Public Economics*, 143:73–88, 2016.

Xiaotian Han, Kaixiong Zhou, Ting-Hsiang Wang, Jundong Li, Fei Wang, and Na Zou. Marginal nodes matter: Towards structure fairness in graphs. *ACM SIGKDD Explorations Newsletter*, 25(2):4–13, 2024.

Moritz Hardt, Eric Price, Eric Price, and Nati Srebro. Equality of opportunity in supervised learning. In *Advances in Neural Information Processing Systems*, volume 29, pages 3315–3323. Curran Associates, Inc., 2016.

Bas Hofstra, Rense Corten, Frank van Tubergen, and Nicole B Ellison. Sources of segregation in social networks: A novel approach using Facebook. *American Sociological Review*, 82(3):625–656, 2017.

Zeinab S. Jalali, Weixiang Wang, Myunghwan Kim, Hema Raghavan, and Sucheta Soundarajan. On the information unfairness of social networks. In *SIAM International Conference on Data Mining (SDM)*, pages 613–521. SIAM, 2020.

Yaning Jia, Chunhui Zhang, and Soroush Vosoughi. Aligning relational learning with Lipschitz fairness. In *International Conference on Learning Representations (ICLR)*, 2024.

Zhimeng Jiang, Xiaotian Han, Chao Fan, Zirui Liu, Na Zou, Ali Mostafavi, and Xia Hu. FMP: Toward fair graph message passing against topology bias. *arXiv preprint arXiv:2202.04187*, 2022.

Vassilis Kalofolias. How to learn a graph from smooth signals. In *International Conference on Artificial Intelligence and Statistics (AISTATS)*, pages 920–929, 2016.

Jian Kang, Jingrui He, Ross Maciejewski, and Hanghang Tong. InFoRM: Individual fairness on graph mining. In *International Conference on Knowledge Discovery and Data Mining (SIGKDD)*, pages 379–389. ACM, 2020.

Fariba Karimi, Mathieu Génois, Claudia Wagner, Philipp Singer, and Markus Strohmaier. Homophily influences ranking of minorities in social networks. *Scientific Reports*, 8(1):11077, 2018.

Ahmad Khajehnejad, Moein Khajehnejad, Mahmoudreza Babaei, Krishna P. Gummadi, Adrian Weller, and Baharan Mirzasoleiman. CrossWalk: Fairness-enhanced node representation learning. *AAAI Conference on Artificial Intelligence*, 36(11):11963–11970, 2022.

Eric D. Kolaczyk. *Statistical Analysis of Network Data: Methods and Models*. Springer, 2009.

O. Deniz Kose and Yanning Shen. Fair node representation learning via adaptive data augmentation. *arXiv preprint arXiv:2201.08549*, 2022.

O. Deniz Kose and Yanning Shen. Dynamic fair node representation learning. In *IEEE International Conference Acoustics, Speech and Signal Processing (ICASSP)*, pages 1–5. IEEE, 2023.

O. Deniz Kose and Yanning Shen. FairWire: Fair graph generation. In *Advances in Neural Information Processing Systems*, volume 37, pages 124451–124478. Curran Associates, Inc., 2024.

O. Deniz Kose, Gonzalo Mateos, and Yanning Shen. Fairness-aware optimal graph filter design. *IEEE Journal of Selected Topics in Signal Processing*, 18(2):142–154, 2024a.

O. Deniz Kose, Gonzalo Mateos, and Yanning Shen. Filtering as rewiring for bias mitigation on graphs. In *IEEE Sensor Array and Multichannel Signal Processing (SAM)*, pages 1–5. IEEE, 2024b.

Preethi Lahoti, Krishna P. Gummadi, and Gerhard Weikum. Operationalizing individual fairness with pairwise fair representations. *Proceedings of the VLDB Endowment*, 13(4):506–518, 2019.

Anja Lambrecht and Catherine Tucker. Algorithmic bias? An empirical study of apparent gender-based discrimination in the display of STEM career ads. *Management Science*, 65(7):2966–2981, 2019.

Yeon-Chang Lee, Hojung Shin, and Sang-Wook Kim. Disentangling, amplifying, and de-biasing: Learning disentangled representations for fair graph neural networks. In *AAAI Conference on Artificial Intelligence*, volume 39, pages 12013–12021, 2025.

Peizhao Li, Yifei Wang, Han Zhao, Pengyu Hong, and Hongfu Liu. On dyadic fairness: Exploring and mitigating bias in graph connections. In *International Conference on Learning Representations (ICLR)*, 2021.

Yanying Li, Xiuling Wang, Yue Ning, and Hui Wang. FairLP: Towards fair link prediction on social network graphs. In *International AAAI Conference on Web and Social Media (ICWSM)*, volume 16, pages 628–639, 2022.

Xiao Lin, Jian Kang, Weilin Cong, and Hanghang Tong. BeMap: Balanced message passing for fair graph neural network. In *Learning on Graphs Conference*, volume 231, pages 37:1–37:25. PMLR, 2024.

Tingwei Liu, Peizhao Li, and Hongfu Liu. Dual node and edge fairness-aware graph partition. *arXiv preprint arXiv:2306.10123*, 2023a.

Yezi Liu, Hanning Chen, and Mohsen Imani. Promoting fairness in link prediction with graph enhancement. *Frontiers in Big Data*, 7:1489306, 2024.

Zemin Liu, Trung-Kien Nguyen, and Yuan Fang. On generalized degree fairness in graph neural networks. In *AAAI Conference on Artificial Intelligence*, volume 37, pages 4525–4533, 2023b.

Renqiang Luo, Huafei Huang, Shuo Yu, Zhuoyang Han, Estrid He, Xiuzhen Zhang, and Feng Xia. FUGNN: Harmonizing fairness and utility in graph neural networks. In *International Conference on Knowledge Discovery and Data Mining (SIGKDD)*, pages 2072–2081. ACM, 2024a.

Renqiang Luo, Huafei Huang, Shuo Yu, Xiuzhen Zhang, and Feng Xia. FairGT: A fairness-aware graph transformer. In *International Joint Conference on Artificial Intelligence*, pages 449–457, 2024b.

Renqiang Luo, Huafei Huang, Ivan Lee, Chengpei Xu, Jianzhong Qi, and Feng Xia. FairGP: A scalable and fair graph transformer using graph partitioning. In *AAAI Conference on Artificial Intelligence*, volume 39, pages 12319–12327, 2025.

Zihan Luo, Hong Huang, Jianxun Lian, Xiran Song, Xing Xie, and Hai Jin. Cross-links matter for link prediction: Rethinking the debiased GNN from a data perspective. In *Advances in Neural Information Processing Systems*, volume 36, pages 79594–79612. Curran Associates, Inc., 2023.

Jiaqi Ma, Junwei Deng, and Qiaozhu Mei. Subgroup generalization and fairness of graph neural networks. In *Advances in Neural Information Processing Systems*, volume 34, pages 1048–1061. Curran Associates, Inc., 2021.

Jing Ma, Ruocheng Guo, Mengting Wan, Longqi Yang, Aidong Zhang, and Jundong Li. Learning fair node representations with graph counterfactual fairness. In *ACM International Conference on Web Search and Data Mining*, pages 695–703. ACM, 2022.

Masoud Mansoury, Himan Abdollahpouri, Mykola Pechenizkiy, Bamshad Mobasher, and Robin Burke. A graph-based approach for mitigating multi-sided exposure bias in recommender systems. *ACM Transactions on Information Systems*, 40(2):1–31, 2022.

Antonio G. Marques, Santiago Segarra, Geert Leus, and Alejandro Ribeiro. Stationary graph processes and spectral estimation. *IEEE Transactions on Signal Processing*, 65(22):5911–5926, 2017.

Antonio G. Marques, Negar Kiyavash, José M.F. Moura, Dimitri Van De Ville, and Rebecca Willett. Graph signal processing: Foundations and emerging directions (editorial). *IEEE Signal Processing Magazine*, 37(6):11–13, 2020.

Farzan Masrour, Tyler Wilson, Heng Yan, Pang-Ning Tan, and Abdol Esfahanian. Bursting the filter bubble: Fairness-aware network link prediction. In *AAAI Conference on Artificial Intelligence*, volume 34, pages 841–848, 2020.

Gonzalo Mateos, Santiago Segarra, Antonio G. Marques, and Alejandro Ribeiro. Connecting the dots: Identifying network structure via graph signal processing. *IEEE Signal Processing Magazine*, 36(3):16–43, 2019.

N. Meinshausen and P. Bühlmann. High-dimensional graphs and variable selection with the lasso. *The Annals of Statistics*, 34(3):1436–1462, 2006.

Adithya K Moorthy, V. Vijaya Saradhi, and Bhanu Prasad. Ensuring fairness in spectral clustering via disparate impact-based graph construction. *IEEE Transactions on Artificial Intelligence*, pages 1–11, 2025.

Madeline Navarro, Yuhao Wang, Antonio G Marques, Caroline Uhler, and Santiago Segarra. Joint inference of multiple graphs from matrix polynomials. *Journal of Machine Learning Research (JMLR)*, 23(76):1–35, 2022.

Madeline Navarro, Samuel Rey, Andrei Buciuma, Antonio G. Marques, and Santiago Segarra. Fair GLASSO: Estimating fair graphical models with unbiased statistical behavior. In *Advances in Neural Information Processing Systems*, volume 37, pages 139589–139620. Curran Associates, Inc., 2024a.

Madeline Navarro, Samuel Rey, Andrei Buciuma, Antonio G. Marques, and Santiago Segarra. Mitigating subpopulation bias for fair network topology inference. In *European Signal Processing Conference (EUSIPCO)*, pages 822–826, 2024b.

Madeline Navarro, Samuel Rey, Andrei Bucilea, Antonio G Marques, and Santiago Segarra. Joint network topology inference in the presence of hidden nodes. *IEEE Transactions on Signal Processing*, 72:2710–2725, 2024c.

Hamed Nilforoshan, Wenli Looi, Emma Pierson, Blanca Villanueva, Nic Fishman, Yiling Chen, John Sholar, Beth Redbird, David Grusky, and Jure Leskovec. Human mobility networks reveal increased segregation in large cities. *Nature*, 624(7992):586–592, 2023.

Hoang NT, Takanori Maehara, and Tsuyoshi Murata. Revisiting graph neural networks: Graph filtering perspective. In *International Conference on Pattern Recognition (ICPR)*, pages 8376–8383. IEEE, 2021.

Włodzimierz Ogrzyczak, Hanan Luss, Michał Pióro, Dritan Nace, and Artur Tomaszewski. Fair optimization and networks: A survey. *Journal of Applied Mathematics*, 2014(1):1–25, 2014.

Antonio Ortega, Pascal Frossard, Jelena Kovačević, Jose M. F. Moura, and Pierre Vandergheynst. Graph signal processing: Overview, challenges, and applications. *Proceedings of the IEEE*, 106(5):808–828, 2018.

Manjish Pal, Sandipan Sikdar, and Niloy Ganguly. Fair link prediction with overlapping groups. *IEEE Transactions on Computational Social Systems*, 12(3):98–1012, 2024.

John Palowitch and Bryan Perozzi. Debiasing graph representations via metadata-orthogonal training. In *IEEE/ACM International Conference Advances in Social Networks Analysis and Mining (ASONAM)*, pages 435–442. IEEE, 2020.

Eli Pariser. *The Filter Bubble: How the New Personalized Web Is Changing What We Read and How We Think*. Penguin, 2011.

Bastien Pasdeloup, Vincent Gripon, Grégoire Mercier, Dominique Pastor, and Michael G. Rabbat. Characterization and inference of graph diffusion processes from observations of stationary signals. *IEEE Transactions on Signal Information Processing over Networks*, 4(3):481–496, 2017.

Nathanaël Perraudin and Pierre Vandergheynst. Stationary signal processing on graphs. *IEEE Transactions on Signal Processing*, 65(13):3462–3477, 2017.

Tahleen Rahman, Bartłomiej Surma, Michael Backes, and Yang Zhang. Fairwalk: Towards fair graph embedding. In *International Joint Conference on Artificial Intelligence*, pages 3289–3295, 2019.

Aida Rahmattalabi, Phebe Vayanos, Anthony Fulginiti, Eric Rice, Bryan Wilder, Amulya Yadav, and Milind Tambe. Exploring algorithmic fairness in robust graph covering problems. In *Advances in Neural Information Processing Systems*, volume 32, pages 15776–15787. Curran Associates, Inc., 2019.

Samuel Rey, T. Mitchell Roddenberry, Santiago Segarra, and Antonio G. Marques. Enhanced graph-learning schemes driven by similar distributions of motifs. *IEEE Transactions on Signal Processing*, 71:3014–3027, 2023.

Samuel Rey, Seyed Saman Saboksayr, and Gonzalo Mateos. Non-negative weighted DAG structure learning. In *IEEE International Conference Acoustics, Speech and Signal Processing (ICASSP)*, pages 1–5. IEEE, 2025.

Manoel Horta Ribeiro, Veniamin Veselovsky, and Robert West. The amplification paradox in recommender systems. In *International AAAI Conference on Web and Social Media (ICWSM)*, volume 17, pages 1138–1142, 2023.

Seyed Saman Saboksayr and Gonzalo Mateos. Accelerated graph learning from smooth signals. *IEEE Signal Processing Letters*, 28:2192–2196, 2021.

Aliaksei Sandryhaila and José M. F. Moura. Discrete signal processing on graphs. *IEEE Transactions on Signal Processing*, 61(7):1644–1656, 2013.

Akrati Saxena, George Fletcher, and Mykola Pechenizkiy. HM-EIICT: Fairness-aware link prediction in complex networks using community information. *Journal of Combinatorial Optimization*, 44(4):2853–2870, 2022.

Akrati Saxena, George Fletcher, and Mykola Pechenizkiy. FairSNA: Algorithmic fairness in social network analysis. *ACM Computing Surveys (CSUR)*, 56(8):1–45, 2024.

Santiago Segarra, Antonio G. Marques, Gonzalo Mateos, and Alejandro Ribeiro. Network topology inference from spectral templates. *IEEE Transactions on Signal Information Processing over Networks*, 3(3):467–483, 2017.

Rasoul Shafipour and Gonzalo Mateos. Online topology inference from streaming stationary graph signals with partial connectivity information. *Algorithms*, 13(9):228, 2020.

Harry Shomer, Wei Jin, Wentao Wang, and Jiliang Tang. Toward degree bias in embedding-based knowledge graph completion. In *ACM Web Conference*, pages 705–715. ACM, 2023.

David I. Shuman, Sunil K. Narang, Pascal Frossard, Antonio Ortega, and Pierre Vandergheynst. The emerging field of signal processing on graphs: Extending high-dimensional data analysis to networks and other irregular domains. *IEEE Signal Processing Magazine*, 30(3):83–98, 2013.

Uriel Singer and Kira Radinsky. EqGNN: Equalized node opportunity in graphs. In *AAAI Conference on Artificial Intelligence*, volume 36, pages 8333–8341, 2022.

Yonas Sium, Qi Li, and Kush R Varshney. Individual fairness in graphs using local and global structural information. In *AAAI/ACM Conference on AI, Ethics, and Society*, volume 7, pages 1379–1389, 2024.

Weihao Song, Yushun Dong, Ninghao Liu, and Jundong Li. GUIDE: Group equality informed individual fairness in graph neural networks. In *International Conference on Knowledge Discovery and Data Mining (SIGKDD)*, pages 1625–1634. ACM, 2022.

Indro Spinelli, Riccardo Bianchini, and Simone Scardapane. Drop edges and adapt: A fairness enforcing fine-tuning for graph neural networks. *Neural Networks*, 167:159–167, 2023.

Alexander J Stewart, Mohsen Mosleh, Marina Diakonova, Antonio A Arechar, David G Rand, and Joshua B Plotkin. Information gerrymandering and undemocratic decisions. *Nature*, 573(7772):117–121, 2019.

Ana-Andreea Stoica, Christopher Riederer, and Augustin Chaintreau. Algorithmic glass ceiling in social networks: The effects of social recommendations on network diversity. In *ACM Web Conference*, page 923–932. ACM, 2018.

Arjun Subramonian, Levent Sagun, and Yizhou Sun. Networked inequality: Preferential attachment bias in graph neural network link prediction. In *International Conference on Machine Learning (ICML)*, volume 235, pages 46891–46925. PMLR, 2024.

Davoud Ataei Tarzanagh, Laura Balzano, and Alfred O. Hero. Fair community detection and structure learning in heterogeneous graphical models. *arXiv preprint arXiv:2112.05128*, 2023.

Victor M. Tenorio, Samuel Rey, and Antonio G. Marques. Robust graph neural network based on graph denoising. In *Asilomar Conference Signals, Systems, and Computers*, pages 578–582, 2023.

Dorina Thanou, Xiaowen Dong, Daniel Kressner, and Pascal Frossard. Learning heat diffusion graphs. *IEEE Transactions on Signal Information Processing over Networks*, 3(3):484–499, 2017.

Daniel Ting, Ling Huang, and Michael Jordan. An analysis of the convergence of graph Laplacians. In *International Conference on Machine Learning (ICML)*, volume 27, pages 1079–1086. PMLR, 2010.

Sotiris Tsoutsouliklis, Evangelia Pitoura, Panayiotis Tsaparas, Ilias Kleftakis, and Nikos Mamoulis. Fairness-aware PageRank. In *ACM Web Conference*, pages 3815–3826. ACM, 2021.

Zichong Wang, Charles Wallace, Albert Bifet, Xin Yao, and Wenbin Zhang. FG^2AN : Fairness-aware graph generative adversarial networks. In *Joint European Conference on Machine Learning and Knowledge Discovery in Databases (ECML PKDD)*, volume 14170, pages 259–275. Springer, 2023.

Zichong Wang, Zhibo Chu, Ronald Blanco, Zhong Chen, Shu-Ching Chen, and Wenbin Zhang. Advancing graph counterfactual fairness through fair representation learning. In *Joint European Conference on Machine Learning and Knowledge Discovery in Databases (ECML PKDD)*, volume 14947, pages 40–58. Springer, 2024a.

Zichong Wang, David Ulloa, Tongjia Yu, Raju Rangaswami, Roland Yap, and Wenbin Zhang. Individual fairness with group constraints in graph neural networks. In *Frontiers in Artificial Intelligence and Applications (FAIA)*. IOS Press, 2024b.

Zichong Wang, Zhipeng Yin, Yuying Zhang, Liping Yang, Tingting Zhang, Niki Pissinou, Yu Cai, Shu Hu, Yun Li, Liang Zhao, and Wenbin Zhang. FG-SMOTE: Towards fair node classification with graph neural network. *ACM SIGKDD Explorations Newsletter*, 26(2):99–108, 2025.

Zonghan Wu, Shirui Pan, Fengwen Chen, Guodong Long, Chengqi Zhang, and Philip S. Yu. A comprehensive survey on graph neural networks. *IEEE Transactions on Neural Networks and Learning Systems*, 32(1):4–24, 2021.

Moyi Yang, Junjie Sheng, Wenyan Liu, Bo Jin, Xiaoling Wang, and Xiangfeng Wang. Obtaining dyadic fairness by optimal transport. In *IEEE International Conference on Big Data (BigData)*, pages 4726–4732. IEEE, 2022.

Wenjing Yang, Haotian Wang, Haoxuan Li, Hao Zou, Ruochun Jin, Kun Kuang, and Peng Cui. Your neighbor matters: Towards fair decisions under networked interference. In *International Conference on Knowledge Discovery and Data Mining (SIGKDD)*, pages 3829–3840. ACM, 2024.

Dimitri Yatsenko, Krešimir Josić, Alexander S. Ecker, Emmanouil Froudarakis, R. James Cotton, and Andreas S. Tolias. Improved estimation and interpretation of correlations in neural circuits. *PLoS Computational Biology*, 11(3):1–28, 2015.

Jiaxi Ying, José Vinícius de Miranda Cardoso, and Daniel Palomar. Nonconvex sparse graph learning under Laplacian constrained graphical model. In *Advances in Neural Information Processing Systems*, volume 33, pages 7101–7113. Curran Associates, Inc., 2020.

Chenyue Zhang, Shangyuan Liu, Hoi-To Wai, and Anthony Man-Cho So. Network games induced prior for graph topology learning. In *IEEE International Conference Acoustics, Speech and Signal Processing (ICASSP)*, pages 1–5. IEEE, 2025a.

Hui Zhang, Ming Yan, and Wotao Yin. One condition for solution uniqueness and robustness of both l_1 -synthesis and l_1 -analysis minimizations. *Advances in Computational Mathematics*, 42(6):1381–1399, 2016.

Juntao Zhang, Sheng Wang, Yuan Sun, and Zhiyong Peng. Prerequisite-driven fair clustering on heterogeneous information networks. *ACM on Management of Data*, 1(2):1–27, 2023a.

Wenbin Zhang, Shuigeng Zhou, Toby Walsh, and Jeremy C. Weiss. Fairness amidst non-IID graph data: A literature review. *AI Magazine*, 46(1):e12212, 2025b.

Xiang Zhang and Qiao Wang. A unified framework for fair spectral clustering with effective graph learning. *arXiv preprint arXiv:2311.13766*, 2023.

Yihong Zhang, Takahiro Hara, and Lina Yao. Biased or debiased: Polarization-aware embedding learning from social media knowledge graph. In *International Joint Conference on Neural Networks (IJCNN)*, pages 1–8. IEEE, 2023b.

Lecheng Zheng, Dawei Zhou, Hanghang Tong, Jiejun Xu, Yada Zhu, and Jingrui He. Fair-Gen: Towards fair graph generation. In *International Conference on Data Engineering (ICDE)*, pages 2285–2297. IEEE, 2024.

Zhuoping Zhou, Davoud Ataee Tarzanagh, Bojian Hou, Qi Long, and Li Shen. Fairness-aware estimation of graphical models. In *Advances in Neural Information Processing Systems*, volume 37, pages 17870–17909. Curran Associates, Inc., 2024.

Yu Zhu, Michael T. Schaub, Ali Jadbabaie, and Santiago Segarra. Network inference from consensus dynamics with unknown parameters. *IEEE Transactions on Signal Information Processing over Networks*, 6:300–315, 2020.